ISSN 1746-7659, England, UK
Journal of Information and Computing Science
Vol. 14, No. 1, 2019, *pp*.052-080

A Comprehensive Design of Unmanned Ground Search and Rescue Robot

Hesham Enshasy[1], Ibrahim Al-Badi[1], Qasem Abu Al-Haija[2],
Muath Al-Saleh[1], Abdulrahman Bu-Shalf[1], Abdullah Al-Dosseri[1]

1 King Faisal University, Department of Electrical Engineering, College of Engineering, Al-Ahsa, Saudi Arabia
2 Tennessee State University, Computer & Information Systems Engineering Department, Nashville, TN, USA
(Received January 13, 2019, accepted March 12, 2019)

Abstract: Rescue workers and fire fighters' job mostly require entering to disaster zones such as factories accident areas, collapsed mines, or burned buildings to perform rescue operations. In addition to human caused disasters, the aftermath of natural disasters such as tornados, earthquakes and tsunamis requires them to be present in order to contain the disaster, help injured victims, and guide trapped victims to a safe exit. The lives of the rescue workers and fire fighter are always at risk in such accidents, since they have no prior knowledge of accident source, environment, and location. Thereby, Search and Rescue Robot (SRR) is an excellent alternative, in which it can perform certain tasks of rescue workers and fire fighters without endangering their life. In a case of disaster, SRR can be sent directly to the danger zones to navigate and provide helpful information regarding the cause of the accident, location of the hazard spots, number of trapped or injured victims, the conditions inside the danger zone, and several other functions. The use of SRR will improve the quality of rescue missions because it can provide important data from the heart of the accident where it is too risky for human to go in. In addition, it can identify the number and the status of the trapped victims and even supply basic equipment, which in some cases can be lifesaving, such as masks and fire blankets in accident which include fires. In this project we designed and fabricated a prototype of search and rescue robot that can perform multiple tasks and can navigate in rough surfaces. The SRR can be controlled from a distance station where the operator can manipulate the SRR movement and its grapping arm while monitoring the surrounding environment using video camera and different sensors. The fabricated prototype successfully passed all the tests that was set to examine its performance.

Keywords: Arduino Microcontroller, Search and Rescue Robot, Geared DC motors, lightweight design, H-bridge module, MQ-Sensors, First Person View (FVP) camera.

1. Introduction

The rapid growth of petrochemicals industry and manufacturing sectors have increased the potential of industrial accidents that could be the result of natural disasters, negligence or incompetence [1]. The scale and number of industrial accidents and natural disasters is unpredictable and even with the strictest precautions, they are still a major threat. There are several types of industrial accidents, which include chemical explosions, mines explosion or collapsing, fires, and chemical leaks. These disasters result in major damages to human lives and properties. In such cases, it is necessary to contain the accident and reduce the damages. Response to an accident or a disaster is always a race against the time. Thus, quick interventions must take place in order to save as much lives as possible and to prevent further damages. Hence, many devoted solutions were shown up in to mitigate these problems such as the development of Search and Rescue Robot. Recently, robotics became a prosper science since many companies and governments are interested in investing in this emerging technology. This resulted in huge robotics research development in which various types of robots were introduced with various characteristics. Moreover, countless features and components were implemented in the designs aiming toward a more practical, intelligent, and efficient robotic systems. Motion is one of the main characteristics of modern robots. In addition, sensory systems allowed scientists and engineers to create more intelligent robots, in which they are capable of sensing physical phenomena. Many sensory systems are available now and can be implemented easily in robots, e.g. rangefinders, ultrasonic, infrared, temperature, gas, distance, and proximity.

Search and Rescue Robot (SRR) is designed to be sent inside the danger zones prior sending the rescue team to explore the area and provide valuable information for them which helps the rescue team to

plan more effective and organized rescue mission. Certainly, SRR will not replace the human rescue workers since humans have a better and faster decision making and actions in critical conditions, however, SRR and rescue workers can work cooperatively in order to perform quality rescue mission. Accident may result in various damages such as building collapse, explosions, harmful gases leakage, fires, and a risk of high temperature through fires. As a result, rescue process is extremely dangerous in such cases without prior knowledge of the accident environment. Furthermore, heavy machinery, which is used to remove the collapsed buildings, cannot be used near an accident site, since the mass of the machinery may disturb the structure of the location and cause further damages. As a result, SRR can be deployed for structural inspection to help the rescue workers avoid actions, which may cause a second collapse. Industrial accidents, which include gas leakage, are another hazard risk because some gases are extremely toxic and flammable. Without a prior knowledge of the presence of such gases, rescue team may suffer bad consequences. The size and design of SRR allows it to move and navigate freely through rough terrains. It can be equipped with video camera placed on the arm, in order to provide 360º live view of the area. Moreover, the SRR can contain number of gas sensors, which cover the most common toxic and flammable gases expected to be found. A temperature and humidity sensors are good addition to the system that can provide needed information. The combination of sensors and camera provides the rescue team with a good insight of the accident environment. This is an important advantage of using SRR, because it allows the team to prepare enough manpower, equipment, and supplies for their rescue mission. The design criterions of SRR (such as size, platform, and features of the robot) are largely influenced by the disaster and function. Consequently, each type of SRR can provide a variety of information according to the working conditions and position. There are three main categories of SRR: Unmanned ground vehicle (UGV), Unmanned aerial vehicles (UAVs), Unmanned underwater vehicles (UUVs). Fig.1. demonstrates Illustration Examples of UGV, UAV, UUV respectively which can be used for different types of search and rescue missions [2, 3, 4]. UGV is a land-based vehicle that operates without the presence of a human on it. They are used in situations where it is dangerous or inconvenient for a human to be onboard. Usually it is remotely controlled from a distant control base, in which all the information communicated or captured by the UGV is sent to the control base. UGVs usually divided into large UGVs and small UGVs. The large UGVs are used to remotely remove large objects such as rocks or rubble. The small UGVs are used mainly for research purposes since they can easily access places that are too small or extremely dangerous. They can perform wide variety of tasks such as finding the location of trapped victims and communicating with them, measuring level of gas leakage/radiations, and capturing live videos. While UAV (drones) is an aircraft that is remotely controlled and widely used for military, inspection, and search and rescue purposes. They can provide a wide coverage of live video or photographs on a certain area from high altitude. In addition, UUVs are unmanned vehicle, which operates underwater. These vehicles are capable of diving underwater and provide valuable information, such as live video, temperature, pressure, and depth. They are employed in rescue operations for marine accidents.

Fig.1. Illustration Examples of UGV, UAV, UUV respectively

In this paper, we propose a complete microcontroller-based design of UGV-SSR, that can offer a great assistance for rescue workers. It can be sent to areas where man can't enter for search and rescue purpose. The robot must navigate its way, sending useful information to the control base and it should be able to perform certain tasks, such as rescue a human, take certain samples from the environment, carry light load and/or run a process in the designated area. The proposed SSR provides wide range of services that are demonstrated in Fig. 2. This diagram shows the wide range of services offered by the proposed design to mitigate risky issues of rescue workers since they are subjected to major and unpredictable hazards such as fires, explosions, and mines or buildings collapsing. For example, the proposed SSR can measure the common dangerous gases in mines and petrochemical facilities [5] such as Methane (CH4), Ammonia (NH3), Liquid Petroleum Gas (LPG), and Carbon dioxide (CO2).

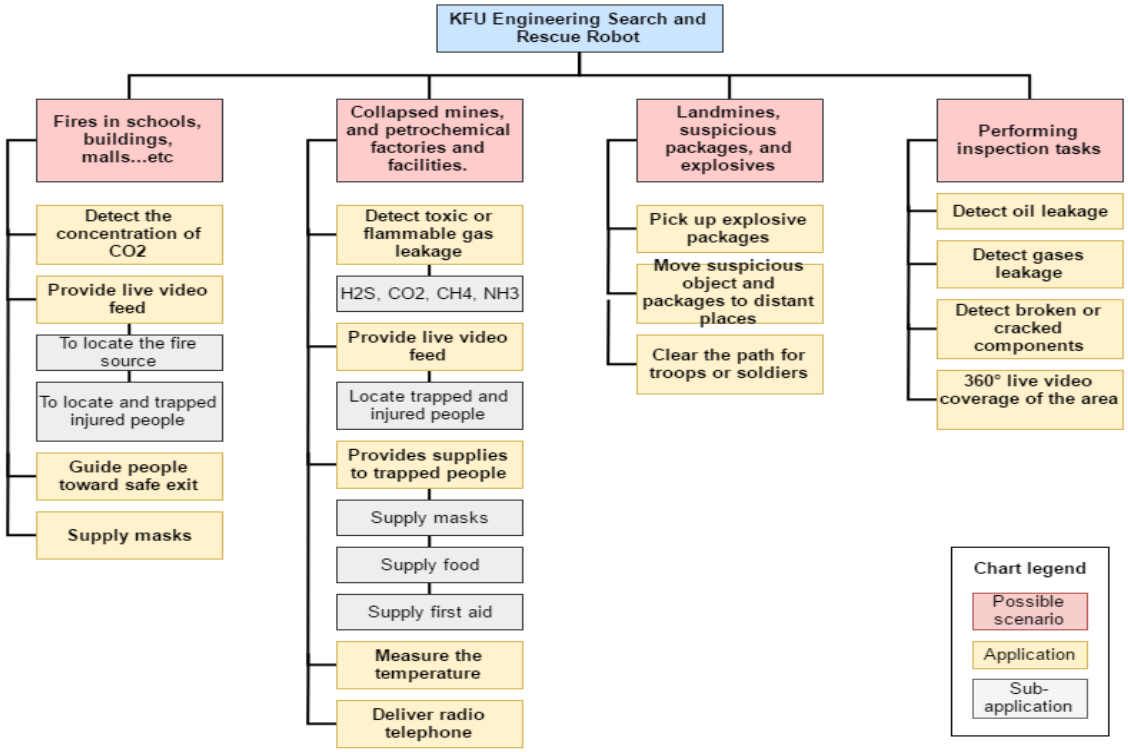

Fig.2. Scenarios where Search and Rescue Robot (SRR) can offer a great assistance.

2. Design Factors and Preliminaries

The dependence on robotic system has been increasing over time and has been replacing humans in various fields. They are used to perform repetitive jobs as in factories and assembly lines. They operate continuously and require minimum human supervision, which improve the productivity of the factory. Therefore, many people are concerned with robotics replacing humans. However, robots are only taking over routine jobs, which many people find it boring. Furthermore, robots are disposable and replaceable, thus, they are used in hazardous and dangerous missions. The use of robots in such scenarios protects human, in fact, in many cases, the use of robot has more advantages than humans. One of the most well-known robots is Curiosity rover, which was sent to Mars back in 2012. The robot, manufactured by NASA, is still in operation today. It provides numerous information about the plant condition. It can take pictures, analyze soil, and measure gas contents in the atmosphere. Such missions are not possible yet to be performed by humans because humans require certain living conditions, whereas robots can operate in various conditions [6].

2.1. Engineering Standards

During the design process, engineering standards which regulate the use of electronic equipment were taken into considerations, especially the radiative equipment, such as Federal Communications Commission (FCC) Standards which used in our design for remote-control transmitter and the transceiver module. Therefore, FLYSKY i6x was tested by the manufacturer and found to comply with class B digital devices. Class B digital device: “A digital device that is marketed for use in a residential environment notwithstanding use in commercial, business and industrial environments. Examples of such devices included, but are not limited to, personal computers, calculators, and similar electronics devices that are marketed for use by the general public. [7]”. The remote control used in this project complies with part 15 of the FCC standards which states that: The device must not cause harmful interference and the device must accept any interference received, including interference that my cause undesired operation. In addition to the remote control, the 433MHz transceiver module also complies with the FCC standards. The US Federal Communications Commission (FCC) regulates operation at 433 MHz under Regulation 10CFR47 Part 15.231 [7].

2.2. Design Specifications and Constraints

To build up a robotic system, the design constrains, and specifications must be set prior to the implementation phase. The constrains and specifications are guidelines which provides physical, logical, and environmental limitation to the design. Table 1 demonstrates the proposed design constrains and the design specifications of the proposed SSR robot.

TABLE 1: DESIGN CONSTRAINS AND SPECIFICATIONS.

Design Variable	Proposed Design Constrains
Dimensions	■ Width: ≤ 60 cm, Length: ≤ 70 cm, Height: ≤ 60 cm. The robot dimensions must be suitable and compatible to maintain stability to enter relatively (small) regions and to carry and store small objects simultaneously.
Mass	■ Total robot mass: ≤ 20 kg, Battery mass: ≤ 5 kg, Able to store supplies of ≤ 1 kg. ■ The mass has a significant impact on the performance and power consumption of the robot, since the heavier the robot, the more torque and power required to move
Power	■ Power consumption: ≤ 200 W. Its battery powered; therefore, it must maintain low power consumption.
Battery	■ Operation time: ≥ 30 minutes. ■ Voltage: 12V, Output current: enough to with stand the components current draw. ■ Dimensions: Small enough to fit inside the robot.
Functions	■ Navigate in rough terrains ■ Collect samples ■ Transmit live video to base ■ Provide useful information.
Arm	■ Mass: ≤ 1 kg and Length: ≥ 60 cm, ■ Must be able to collect samples. ■ Samples mass: ≤ 100 gm, ■ Degrees of freedom: ≥ 3. ■ Arm must be able to move freely in all directions and collect samples. ■ A camera must be attached to the arm which must have suitable length to pick up samples from the ground
Motors	■ Moderate speed: ≥ 40 RPM, ■ Number of motors: 2 motors ■ Torque: enough to push the robot. ■ Small size, ■ Mass: ≤ 1 kg per motor.

General Specifications		Mechanical Specifications	
Robot Category	UGV: Search and rescue	Total height	43 cm
Arm	3 DOF arm with a gripper.	Total width (without tracks)	50 cm
Remote controlled	2.4GHz remote control system.	Total width (with tracks)	45.5 cm
Sensory system	Gas, temperature, humidity, distance.	Total length (without arm)	55 cm
Battery	12V, 18 Ah, Operates up to 94 minutes.	Arm length	67 cm
Wireless Comm./ Camera	Available	Robot estimated mass (without supplies)	14.6 kg
Electrical Specifications		Supplies storage capacity	1 kg
Microcontroller type	Vehicle propulsion	Vehicle propulsion	Continuous
Number of microcontrollers	Number of motors	Number of motors	2 (left/right)
System voltage	Speed	Speed	54 rpm
System total power	Required torque	Required torque	2.53 Nm
Required battery capacity	Available motor torque	Available motor torque	4.41 Nm
Available Battery capacity	18 Ah	Motor power	25 W
Wireless comm. frequencies	433MHz, 2.4GHz, and 5.8GHz	Number of sensors	6

2.3. Design Alternatives

There are three different design alternative that can be considered at the implementation stage of this work:

- Design Alternative I: Robot with regular wheels could be used. This design is the easiest and has the lowest cost. However, such a robot is not suitable for all types of lands. In soft soils, due to the high ground pressure on the wheels, the wheels can easily get stuck in the soil.
- Design Alternative II: Two arms could be implemented instead of one, which is not efficient, since one arm is enough for the robot. Implementing two arms would make the control process through a remote control very complicated. It will also lead to an increase in the mass and the cost.
- Design Alternative III: Walking robot with four legs, which offers an ability to navigate through different terrains. It has an extremely complex design and required expensive components, such as hydraulic actuators and lightweight material for the body such as: carbon fibers.

In this work, we have selected to implement the design alternative I due to its advantages over other design in terms of size, mass, and cost. The total cost to build up this design is about 1100$ including all parts.

3. Mechanical Design of SSR

The search and rescue robot must be able to drive through rough and uneven terrains. Therefore, it must be able to maintain a proper center of gravity. In this work, this was achieved by the evenly

distribution of the robot weight at each side of the robot. The height of the robot was reduced, and the width of the robot was increased which allows the robot to have more ground contact and stability while driving in uneven terrains. If the robot was an adequately high, slight inclinations could affect the balance of the robot and make it fall. The design of the robot is like a tank with continuous tracks as the driving mechanism. Fig.3. demonstrates the robot's structural design including key specifications and dimensions.

3.1. Raw Material

In order to choose a construction raw material; it must be suitable for the purpose of the project. Since the aim of this project is to design a search and rescue robot whose main function is to search and explore, it is necessary for the robot to consume minimum power, in addition to have a metallic, rigid and strong structure. Several metals were suggested and investigated such as: steel, aluminum, galvanized iron. However, after researching and testing, aluminum was chosen since it serves the purpose of the project and it has several advantages over other materials. Aluminum is one of the most common construction materials for robots, since it is strong, durable, lightweight, and not expensive. The mass of the robot has a huge impact on the power consumption and the size of motors. Aluminum has an excellent strength-to-mass ratio which makes it suitable for such applications that require mobility and low power consumption [8]. Table 2 demonstrates a comparison between aluminum and steel, and in which most of the parameters are in favor of aluminum.

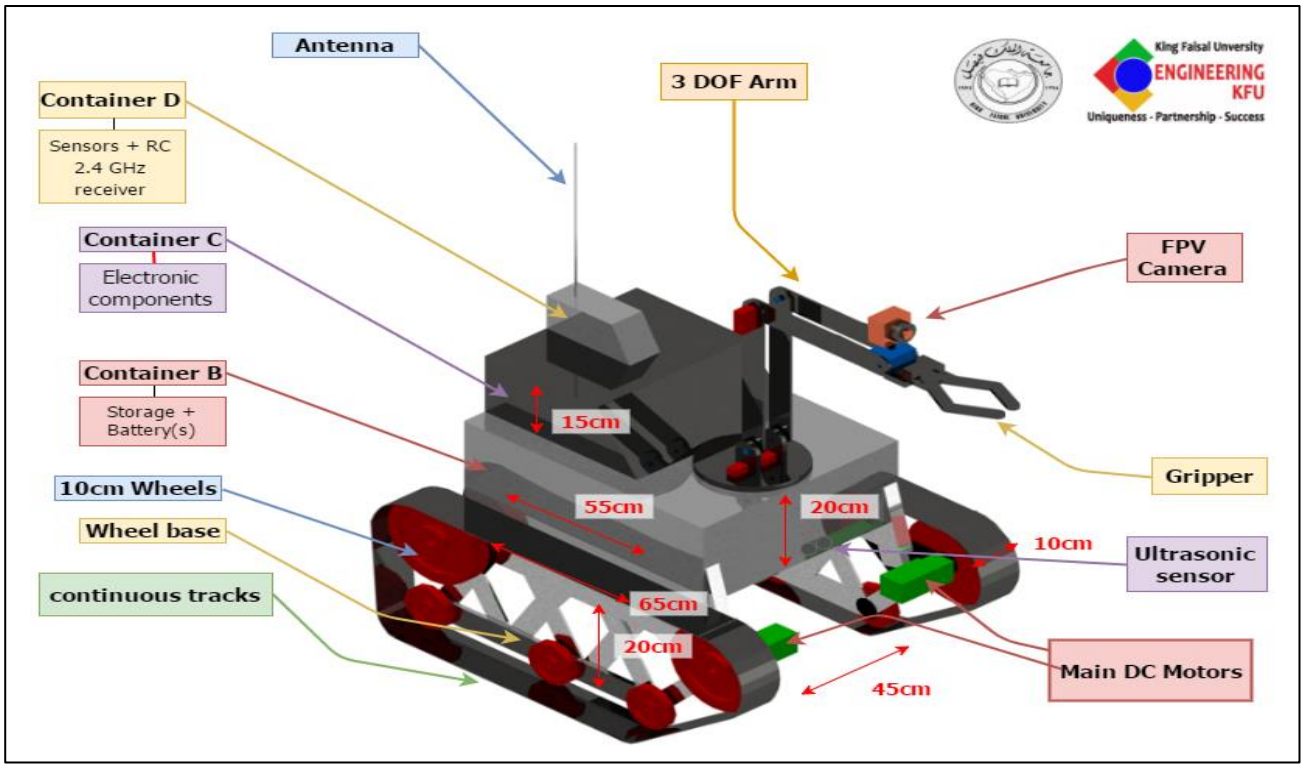

Fig.3. Robot conceptual design with description.

TABLE 2: COMPARISON BETWEEN ALUMINUM AND STEEL AS ROBOT BUILDING MATERIAL.

Parameter	Aluminum [8]	Steel [9]
Material type	Chemical element	Alloy Mixture of iron, carbon, chromium
Density	2.70 g/cm^3	7.85 g/cm^3
Moh's hardness	2.75	4-4.5
Brinell hardness	15 HB	121 HB
Strength	Good	Very strong
Mass	Very light	Heavy
Corrosion resistance	Yes	Yes
Price	Medium	More expansive
Workability	Easy to cut/form/shape	More difficult

DOI https://doi.org/2024-JICS-22432 | Generated on 2025-04-05 22:12:07

By knowing the density of the material, it is possible to estimate the mass of the aluminum plates and number of the needed plates which will be used in the robot using the formula [10]: $\boldsymbol{M = \rho * v = \rho\,(a * b * c)}$. Where, $\boldsymbol{M}$: mass of the plate, $\boldsymbol{\rho}$: density of the material. For a plate $\rho = length * width * thickness$, $\boldsymbol{a}$: length of the plate, $\boldsymbol{b}$: width of the plate, $\boldsymbol{c}$: thickness of the plate. Thus, Table 3 demonstrates the dimension and mass of each body part of the robot.

TABLE 3: THE ROBOT BODY ALUMINUM PLATES MASS.

Main Part	Sub part	a (cm)	b (cm)	c (mm)	ρ (g/cm^3)	No.	Mass (kg)
Container B	B1	55	45	1	2.7177	2	1.345
	B2	55	20			2	0.598
	B3	20	45			2	0.489
Container C	C1	40	30			1	0.326
	C2	40	15			2	0.326
	C3	15	30			2	0.245
Container D	D1	7	15			1	0.029
	D2	7	5			2	0.020
	D3	5	15			2	0.041
Legs		30	5	4		4	0.326
Bolts		-	-	-		-	0.400
Wheel Base	WB1	50	4	2		2	0.283
	WB2	60	4			2	0.261
Misc. Parts		15	4			8	0.261
Total mass							4.950

Similarly, we calculated the mass of the arm which is necessary to determine the torque of joint motors later. Table 4 demonstrates the dimensions of the arm components along with their masses.

TABLE 4: THE MASSES IF ALUMINUM PLATES OF THE ARM.

Main part	Sub part	a (cm)	b (cm)	c (mm)	ρ (g/cm^3)	No.	Mass (kg)	Mass (kg) 120%
Arm	Joint 1 (45*5)	45	5	1	2.7177	2	0.123	0.147
	Joint 2 (35*4)	35	4			2	0.076	0.092
	Gripper	-				1	0.100	0.120
Arm Base		10cm diameter – 2 cm high				1	0.214	0.257
Total							**0.513**	**0.616**

3.2. Coupling and Bearings

One of the mechanical parts is a coupling and it is used to transfer the rotation and the torque. The coupling is used to conjoin other parts with rotor part of the motor which cannot be connected right away because of the distance. Also, to insert a driving wheel with the motor, we need to extend the shaft from the motor side and connect it to the coupling. Then, the driving wheel will rotate smoothly. The bearing is a mechanical component that is used to provide a smooth movement and it is also reduces the fraction between the moving parts. For this design, a bearing with free rotation around fixed rod will be used in the construction of the arm. Fig. 4. shows: (a) the coupling shaft to link the motor with the wheel, (b) the bearing used in our design and (c) the motion system [9]. Moreover, bearings will also be used for the remaining wheels which are not connected to a motor, in which it allows for a smooth rotation.

Figure 4: (a) Coupling shaft. (b) The used bearings (c) Motion system

3.3. Continuous Track

The SRR is to be equipped with a ground vehicle propulsion system, which can be either regular wheels or continuous tracks. Both systems offer unique features and advantages when used with certain terrains. The first step in determining the suitable vehicle propulsion system is to determine in what terrains

this robot be used. As for our design, we are focusing on cruising through rough terrains, sandy lands, and soft-soil lands. Also, it must be able to overcome rubbles, small objects and obstacles. Ground pressure is the force applied by an object on the ground. This is an important concept for vehicles intended to be used on sandy areas or soft-soils. The higher the ground pressure, the harder for the object to maintain mobility on the surface. The contact area of the object plays a significant role in determining the ground pressure [11]. The general formula for pressure is given by $\boldsymbol{P = F/A}$. This formula represents the ground pressure for idealized case, where the force is divided by the area. Thus, increasing the area of contact will reduce the ground pressure. Therefore, instead of using regular wheels which have smaller surface area, continuous track system could be used which has a much higher surface area. Because continuous track system has a larger contact area, it has lower ground pressure too; thus, it is suitable to be for sandy areas, and soft-soil lands. In addition, continuous-tracks system provides smoother drive on harsh terrains and different soil conditions, since it has a higher ground traction and continuous ground contact. Continuous track system offers a better maneuverability, where it allows the robot to rotate even when it is stationary [11].

Fig.5. (a) 5 cm diameter tank driving wheel (b) Implementation of driving wheel & continuous track(c) Supporting wheel

Taken into consideration the design constrains of the robot, the length of the robot (with tracks) is assumed to be 65 cm, and the tracks width to be 20 cm. Moreover, wheel diameter impacts the motors torque significantly, where wheels with large diameters required more torque. Thus, the wheel diameter is assumed to be 10 cm. The driving wheels are to be surrounded by the tracks, thus, two 5 cm wheels along with three 5 cm diameter wheels will be used at both sides. The selected wheels and tracks are demonstrated in Fig.5. through (12) along with their specifications in Table 5.

TABLE 5: DRIVING WHEELS, CONTINUOUS TRACK, AND SUPPORTING WHEELS SPECIFICATIONS.

Parameter	**Driving wheel**	**Supporting wheel**	**Track**
Width	4 cm	4 cm	4.5 cm
Diameter	5 cm	5 cm	5 cm
Mass	115 g	45 g	84 cm
Material	Aluminum	Aluminum	Plastic

Furthermore, the continuous track needs supporting wheels, which rotate freely. These supporting wheels provide the necessary tension to the track. Fig.5 shows the supporting wheel chosen for the project. We have used five supporting wheels support the track and form the front and rear angles which helps in driving over obstacles. Also, the ground pressure depends on the area of the wheels and track. Fig.6 shows the parameters of both cases.

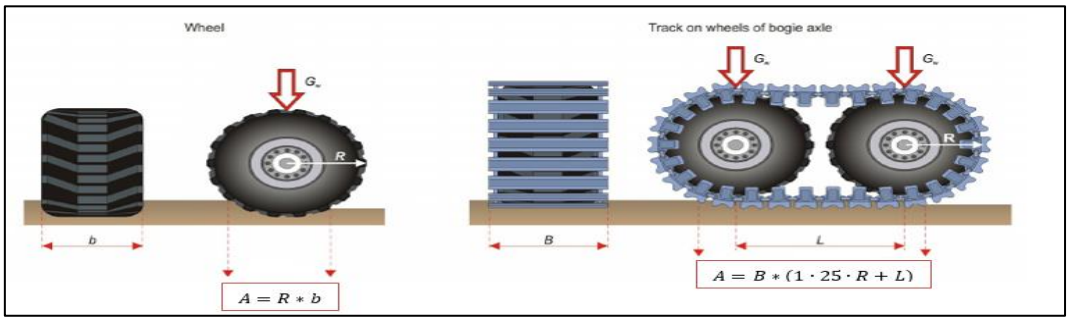

Fig.6. Nominal ground pressure parameters for wheel & tracked wheels.

Given that GW: Wheel mass, A: Wheel area, R: Unloaded wheel radius and b: Width of tire. Then, the formula to calculate the Nominal Ground Pressure for a wheel [12] is given by:

$$NGP = \frac{G_w}{A} = \frac{G_w}{R * b} \quad \xrightarrow{Therefore} \quad NGP = \frac{(115 * 10^{-3})}{\left(\frac{10}{2}\right) * 4} = 0.00575\ kg.cm^{-2}$$

Also, assume that Gt: track mass, B: width of the tracks and L: the distance between the two wheels' center. Then, the nominal ground pressure for track on wheel of tracked wheels is given by the formula [12]:

$$NGP = \frac{(2 * G_w) + G_t}{A} = \frac{(2 * G_w) + G_t}{B * (1.25 * R + L)} \quad \xrightarrow{Therefore} \quad NGP = \frac{(2 * 115 * 10^{-3}) + 1}{(10) * [1.25 * (5) + (65)]} = 0 \cdot 0017263\ kg\ .cm^{-2}$$

It is obtained from the calculation that by using regular wheels, the ground pressure on the wheel will be as high as 0.00575 kg.cm-2, compared to continuous track which has ground pressure of 0.00173 kg.cm-2. The following calculations are for the actual wheels and tracks used in the project.

$$NGP = \frac{(2 * 270 * 10^{-3}) + 1}{(4.5) * [1.25 * (4.75) + (38.5)]} = 0.0077012\ kg\ .cm^{-2}$$

It is observed that the ground pressure is 0.0077012 kg.cm-2. This value is suitable since we have used 5 supporting wheels. Although the ground pressure of the tracked wheels is little bit higher, it introduces more advantages than regular wheels.

3.4. Robotic Arm

When designing the robotic arm, two main factors must be taken into consideration, which are degrees of freedom and the required torque in each joint of the arm. The degrees of freedom are very important concept to understand. Each degree of freedom is a joint on the arm, where it contains an actuator that rotates the joint. Thus, the number of degrees of freedom is usually equal to the number of actuators on the robot arm. In general, it is preferred to reduce the number of degrees of freedom in order to reduce the cost and construction complexity [13]. Fig.7. (a) illustrates the proposed arm design for the project, which has 3 degrees of freedom. For every joint in the arm, an actuator must be present in order to provide the rotation. However, it is necessary to calculate the torque required by each actuator that can withstand lifting a certain mass including the mass of rest of the arm. In this prototype arm, servo motors will be used in the joints, since servo motors have two advantages over other actuators: they are easier to control and more accurate, they come in small sizes that make them easy to integrate, and they come with high torques. The most common units for servo torque are KG-CM, which is equal to 0.0980665 N-m [14]. Therefore, in order to ensure proper and smooth motion of the arm, the torque for each servo must be calculated during the design of the arm. The torque is also influenced by the length of each link in the arm; the longer the arm, the more torque is required.

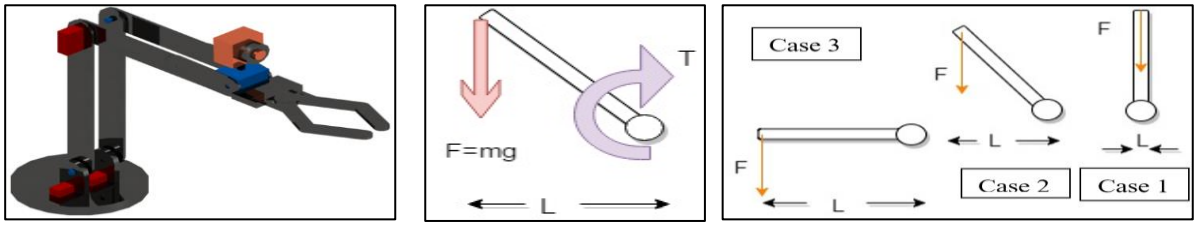

Fig. 7. (a) Basic design of the 3-DOF robotic arm (b) The relation between torque and length. (c) the possible cases of a link position

Torque (T) is defined as the force required to make an object rotate and it is calculated using the formula: $\boldsymbol{T = F \cdot L}$. On a vertical plane, the force pulling the object downward is due to gravity acceleration g. Therefore, to find the value for this force, the mass of the object is multiplied by g which is equal to 9.81m/s2 as shown in the equation: $\boldsymbol{F = w = m \cdot g}$. Thus, the required torque to hold a mass at a certain distance from the pivot point as shown in Fig.7 (b) is given by: $\boldsymbol{T = m \cdot g \cdot L}$. To calculate the torque required at each servo motor, the calculation must be done for the case where maximum torque is required. It is observed from fig.7 (c) that maximum torque is required when the force is perpendicular to the joint as in case 3. Note that in the figure, it is desired to rotate the joint clockwise. As for L1 case, we have the shortest distance and by multiplying by the force, we obtain the lowest value. However, for L3, by multiplying the length by the force, we obtain the highest value. The weight of the link must be considered, and it located roughly at the center of mass of the link, thus, it is multiplied by half the length of the arm.

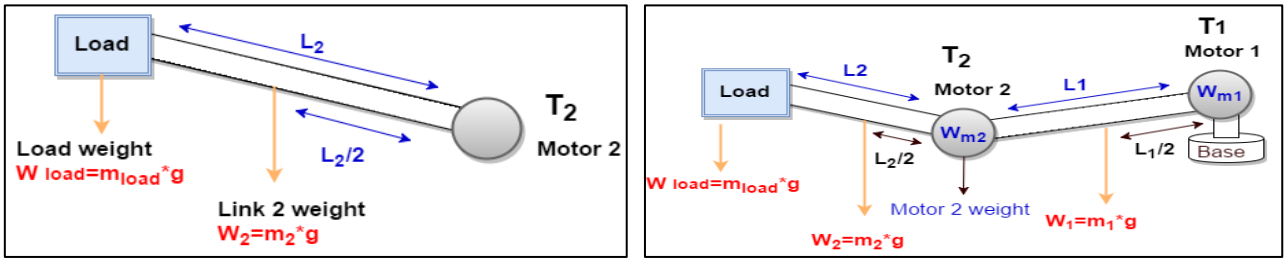

Fig.8 The torque required by (a) one motor to rotate a link with an object (b) for multiple joints arm

Also, the mass of the held object is multiplied by the length of arm, since the object will be located at the end of the arm as demonstrated in fig.8(a). The pervious values are then added to obtain the torque required by servo motor 3 to rotate one link and an object as expressed in the following relation: $T_2 = (w_{load} * L_2) + (w_2 * L_2/2)$. This formula is then used to calculate the servo required to lift the closest link to the load. However, to find the required torque to lift the entire arm, the same principle is applied as shown in fig.8(b). Thus, the required torque (T_1) for motor (2) is derived as follows:

$$T_1 = (w_{load} * (L_1 + L_2)) + (w_2 * (L_1 + L_2/2)) + (w_{m2} * L_1) + (w_1 * L_1/2)$$

It is observed that by increasing the degrees of freedom, the number of servo motors and the complexity of the calculations will increase too. The mass of the arm plates was estimated earlier, and now it will be used to determine the torque of each servo motor. The equation was implemented into MS excel to calculate the needed torque directly. Fig.9 demonstrates the arm design along with the dimensions. It has three joints, hence, three degrees of freedom. Moreover, a gripper or a claw which will be used for picking up items will be implemented. To provide the ability to control the camera view and allow for 360-degree coverage, the camera will be installed on top of the gripper as demonstrated.

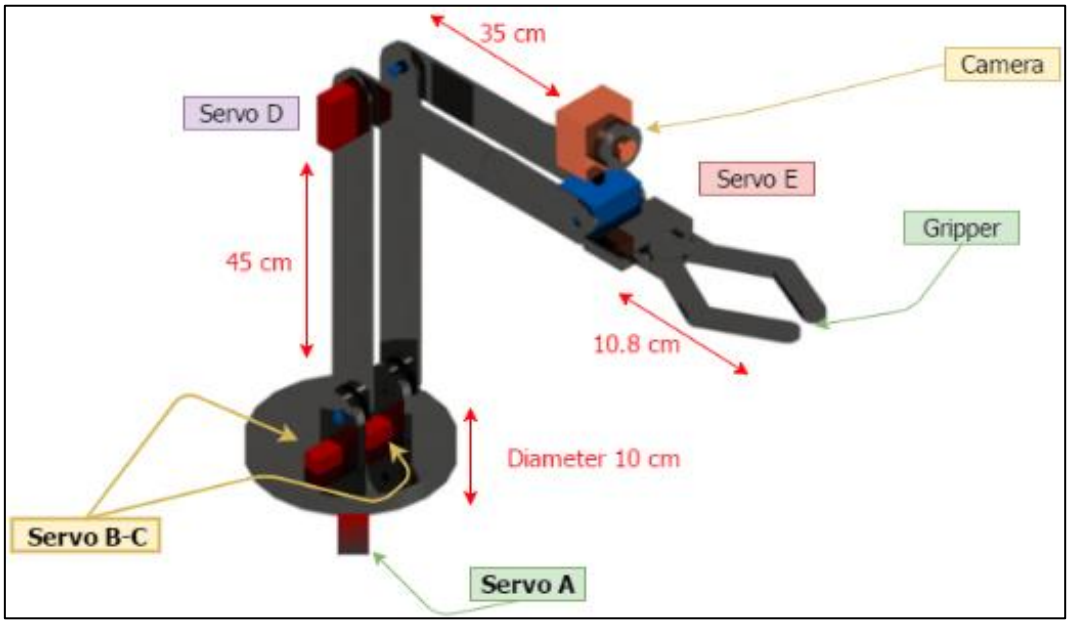

Fig.9. Dimensions and labels of the designed robotic arm.

The mass of the arm joints was calculated previously, therefore, we can use formulas 3 and 4 to calculate the required torque to lift the arm are demonstrated in Table 6.

TABLE 6. TORQUE CALCULATIONS FOR THE ARM SERVO MOTORS.

Part	Mass (kg)	Sample ass (kg)	Required Torque (KG-CM)	Corresponding servo
20 cm diameter Base	0.035	-	5.00	A
Long link 45×5	0.147	-	28.88	B+C
Short link 35×4	0.092	-	9.959	D
Gripper	0.120	0.1	1.350	E
Camera	0.002	-	-	-

Later, in the construction process, some changes in the shape and mechanism of the arm were made in order to enhance the performance. A 15 kg-cm torque servo motor is available with reasonable price.

DOI https://doi.org/2024-JICS-22432 | Generated on 2025-04-05 22:12:07

Therefore, B and C servos will have a torque of 15 kg-cm each accumulating a total torque of 30 kg-cm which is enough for our application. Furthermore, for servo A and D, a torque 5 kg-cm and ~10 kg-cm respectably is required. After researching, it was found that such servos with such parameters are either not available or expensive. In addition, the 5 kg-cm servo has plastic gears rather than metallic, where plastic gears can be damaged easily. Thus, due to the availability and convince of the 15 kg-cm servo, it was decided to use this parameter for the A, B, C, and D servos. Note that the 5 kg-cm, 10 kg-cm and, 15kg-cm have approximately mass of ~56 grams, therefore, the arm will have a higher torque capability with no extra mass or price. Note that an FPV camera will be installed on the arm, which has a negligible mass of 15-25 grams. Furthermore, 20 kg.cm servos were bought later to replace servos B and C which have 15 kg.cm torque, in order to provide the arm with better performance. Thus, the base servos have a total torque of 40 kg.cm. Table 7 demonstrates the compression between several servos which the team considered. According to the table, we have considered two types of servos: HDKJ D3615 and PDI-6221MG, since they have more advantages in terms of torque and price. Also, both motors require the operational voltage of 7.4 V and run at the same speed of 0.16sec/60 degrees.

TABLE 7. COMPARISON BETWEEN THE 5,10, 15, AND 20 KG-CM SERVOS [21]

Name	SG-5010	DM-S0900MD	HDKJ D3615	PDI-6221MG
Torque	5 kg-cm	10 kg-cm	15 kg-cm	20 kg.cm
Gears material	Plastic	Metal	Metal	Metal
Mass	38 g	56 g	56 g	62 g
Price	$12.16	$15.24	$11.39	$ 12.5

The power consumption of the servos must be calculated, since they will be used later to size the battery.

$$1\ \text{N.m} = 10.197162\ \text{kg.cm} \rightarrow 15\ \text{kg.cm} = 1.471\ \text{N.m}$$

$$1\ \text{degree/sec} = 0.16667\ \text{rpm} \quad \text{therefore} \quad 0.16\ \text{sec}/60\ \text{degrees} = 375\ \text{degree/sec} = 65.5\ \text{rpm}$$

According to [15], the power of a DC servo motor is given by $P = T \cdot W$, where, T: torque in N-m and w: speed in Rad/sec, 1 rad/sec = 60/2π rpm = 9.549, then: $P = 1.471\,Nm \times (65.5\,rpm)/9.549 = 10.09\,watts$. Also, the same concept was applied to find the power of the 20 kg.cm servo which is calculated as $13.45\,watts$. This method of power computation is repeated to all the servos of the arm. The results of calculations are listed in Table 8 along with the arm specifications.

TABLE 8. THE SERVO ARM CALCULATIONS AND SPECIFICATIONS.

Servo	Required torque (kg-cm)	Available torque (kg-cm)	Power consumption (w)	Speed (rpm)	Rated voltage (V)
A	5.00	15.00	10.09	65.5	7.4
B	14.44	20.00	13.45	65.5	7.4
C	14.44	20.00	13.45	65.5	7.4
D	9.96	15.00	10.09	65.5	7.4
E	15.00	15.00	10.09	65.5	7.4
Specification of the Servo Arm (7.4-volt servos)					
Motion Range: 0-180°		Number of motors: 5 DC servo motors		Degrees of freedom: 3 (extend, contract, tilt)	
Total length of the arm: 67.5 cm		Total mass of the arm: 0.74 KG		Total power consumption: 57.2 W	

3.5. Estimated Mass

Calculating the mass of the robot is essential to determine the torque needed to drive the motors. In Table 9, all the components of the robot were listed along with their masses. Note that a 20% safety factor was considered to avoid future mass differences. Note that the actual mass of the robot was found to be 14.6 kg (with an empty storage area) compared to the calculated mass of 18.45 kg. As a result, the actual robot is 20.86% lighter than calculated. The robot is lighter because our team have used lighter DC motors and lighter tracks. In addition, the robot frame was made entirely from aluminum, however, it was covered with plastic laminations instead of aluminum. This resulted in noticeable mass reduction.

TABLE 9: COMPONENTS OF THE ROBOT AND THEIR CORRESPONDING ESTIMATED MASSES.

Item	Est. Mass/Pcs (Kg)	No.	Estimated Mass (Kg)
Body	5.00	1	5.00
Tracks	1.00	2	2.00
10 cm rubber wheels	0.115	4	0.46
3-5 cm rubber wheels	0.05	6	0.30
Servos motors	0.056	5	0.28
Arm aluminum plates	0.78	1	0.62
Electronics	0.35	1	0.35
Battery	5.00	1	5.00
Motors	0.68	2	1.36
Theoretical mass			15.37 kg
Theoretical mass + Safety factor (1.2) *(Empty container)*			18.45 kg
Theoretical mass + Safety factor (1.2) + Full container (500gm)			18.95 kg
Actual mass + Battery *(Empty container)*			14.6 kg

3.6. Motors Selection

The motor selection is influenced by several factors, which are speed range, torque, power, starting torque, and operating time. In addition, actuators come in various variations, therefore, to differentiate between the different types of actuators, they are categorized in terms of their torque and rotational speed. DC motors have a high speed in general, and most DC motors have low torque. Therefore, to reduce the speed and increase the torque, gears can be added. To determine the required torque for the motor, several factors must be taken into consideration, such as: mass of the system, maximum incline, wheel radius, and the required acceleration.

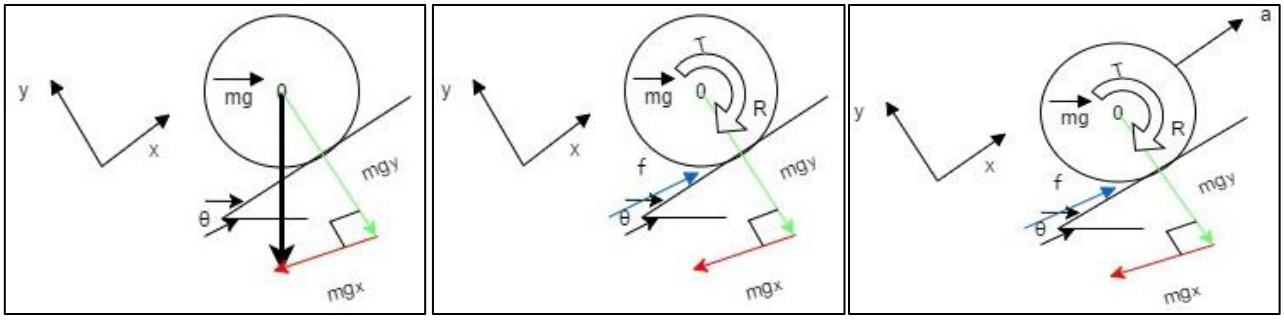

Fig.10. (a) A free body of the wheel. (b) A free body along with torque component (c) A free body along with acceleration component

Fig.10 (a) demonstrates a free body diagram of the wheel, where θ represents the maximum incline angle that the wheel can climb. Mgy and Mgx are the weight components, where the first is parallel to the surface which cause the wheel to move downward, and the second is balanced by the force exerted on the wheels. The components mgy & mgx can be expressed [16] as: $mg_x = mg \cdot sin\theta$ and $mg_y = mg \cdot cos\theta$.Therefore, in order for the wheel to stay positioned or and not to move downward, a friction force must be present as demonstrated in the fig.11(b). Therefore, the torque required to rotate the wheel is expressed as the force multiplied by the wheel radius [23] as shown in the following relation: $T = f \cdot R$. Since the robot have a certain acceleration speed, the acceleration must be considered too, therefore, the acceleration is to be added to the free body diagram as shown in the fig.11(c). Now, all forces (F) are along the x and y axes. We balance the forces in the x-direction as follows: $M.a = f - M \cdot g_x$. By substituting the torque formula ($T = f \cdot R$) in this equation, we obtained the following: $M \cdot a = T/R - M \cdot g_x$. By solving for the torque T, the following relation is obtained: $T = R \cdot M \cdot (a + g \cdot \sin(\theta))$. This formula is used to calculate the torque for one motor. However, if more than one motor is used, this equation must be

DOI https://doi.org/2024-JICS-22432 | Generated on 2025-04-05 22:12:07

divided by the number of motors N as follows: $T = (R \cdot M \cdot (a + g \cdot sin(\theta)))/N$. Where, T: torque, g: acceleration due to gravity, N: number of wheels, M: total mass, R: radius of the wheel, a: acceleration, and θ: incline angel. The final point to consider is the efficiency (e) in the motor, gearing and wheel (slip) then,

$$T = \left(\frac{100}{e}\right) \cdot \frac{R \cdot M \cdot (a + g \cdot \sin(\theta))}{N}$$

The power of a motor is the torque in Nm times the speed in RPM, and it is expended as: $P = \tau \cdot \omega$. The current drawn by the motor is calculated by using the following formula: $I = P/V = (T \cdot \omega)/V$. The Relation between RPM and radian per second: $1\, rev/min = 2\pi/60\, rad/sec$. By plugging the desired parameters into the pervious equations, the results in table (13) were obtained. By substituting the information provided in Table 10 in the last torque formula we found that $T = 2.53\, Nm$. Finally, we observed that the mass of the robot influences the required torque as demonstrated in Fig.11(a) and the torque of the DC motor is oppositely relational to the speed as demonstrated in Fig.11(b).

TABLE 10: THE PARAMETERS AND REQUIRED SPECIFICATIONS OF THE MOTORS.

Parameter	**Theoretical Values**	**Parameter**	**Theoretical Values**
Supply voltage	12 V	Assumed total efficiency	65%
Total mass M (with full container)	19 kg	Assumed Angular velocity	96 RPM
Number of motors	2	Max current	2.11 A
Wheel radius R	0.05 m	Power	17.22 W
Desired velocity	0.05 m/s	Required torque	2.53 Nm

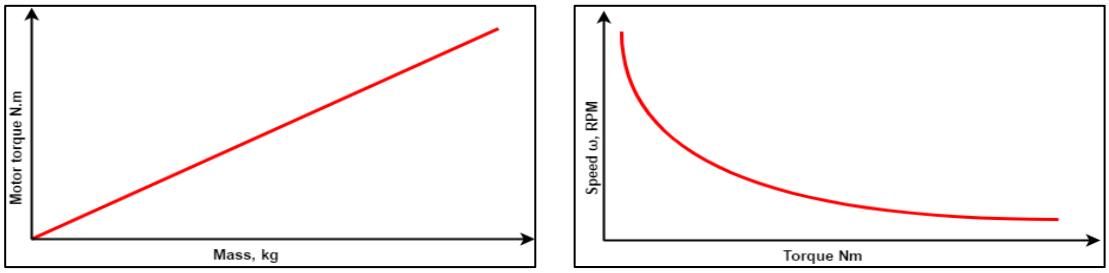

Fig.11. (a) The relation between the mass and torque (b) Torque-speed characteristics of a DC motor.

Note that the power of the motor was not given, however, it was calculated using the torque and speed as follows:

$Given: Torque = 45\, Kg.cm = 4.41\, N.M,\ Speed = 54\, RPM,$ ➔ $Power = (Torque\ (N.M) * Speed\ (RPM))/9.5488 = \mathbf{25\ W}$

The selected motor or our proposed design is the DC brushed motor since it has multiple gears embedded within the motor's enclosure which results in high torque with respect to lower speed. Fig.12 demonstrates the physical shape of the motor along with its specifications. It is observed that the parts of the motor are well protected and enclosed [17]. In addition, the selected motor has better performance in terms of torque and continuous current.

Specification of the selected motor	
Parameter	**Value**
Type	Brushed DC Motor
Rated Voltage	12
Rated Torque	54 kg.cm
Speed	54 rpm
Starting current	1.6A - 2.1A
Continuous current	0.9A - 1.2A
Rated Power	25W

Fig.12. The DC motor components along with its specifications

4. Electrical Design of SRR

Electrically, SRR contains many electronic and electrical components and modules such as multiple sensors, camera and several. The electrical components block diagram of proposed SRR is demonstrated in Fig.13. As clearly seen, two Arduino Uno microcontroller units (MCU) are used on the robot: MCU_A controls the motion parts of the robot and MCU_B controls the sensory system and wireless communication. Such arrangement provides more efficient control system and simplifies programming process, because each system has a separate program. In addition, since the robot encompasses different components with

different voltages to operate, a power regulation unit was constructed. However, the system modules will be discussed in detail in the upcoming subsections.

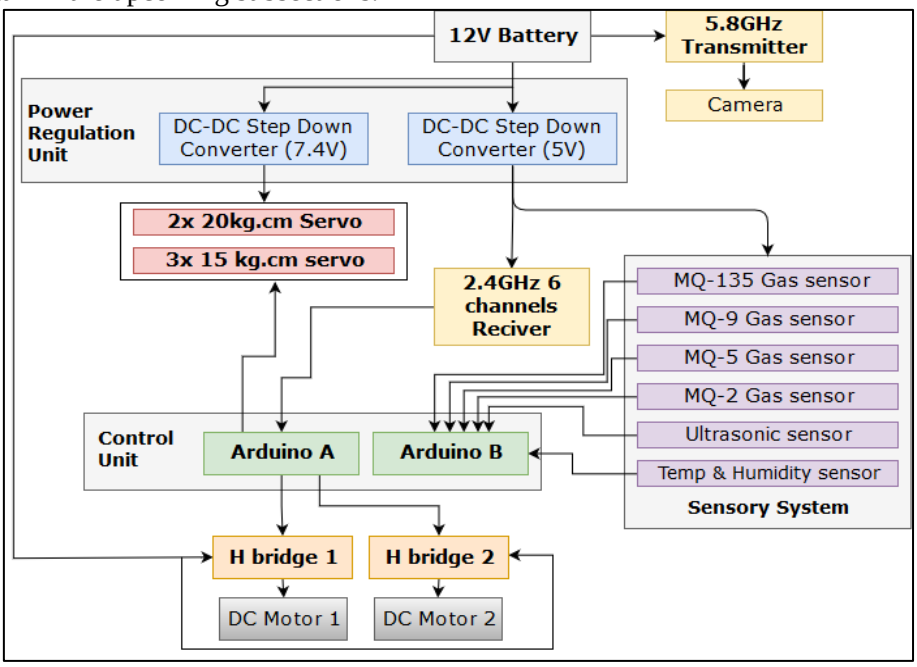

Fig.13. Block diagram of the electrical components.

4.1. Remote Control Unit

A remote control is a device used to control systems wirelessly from a distance. Two types of remote-control systems are commonly used: Infrared (IR) based systems and Radio Frequency (RF) based systems. IR remotes must be pointed directly at the devices to control it, which is not valid for our proposed SRR. While, RF remote can be used from far distance, which is suitable for our case. Unlike the common IR remotes, RF remotes do not have to be aimed at the equipment. RF remote control required RF transmitter and RF receiver, in which both must have the same frequency. In such remote controls, the most common frequency band is 2.4 GHz. In this work, we have used 6-channel RF based FLYSKY FS-i6 operating at 2.4 GHz (illustrated in Fig.14 (a)). The 6-channels allow the user to control 6-different pins at the receiving end. Each channel at the transmitter controls one function only at the receiver as demonstrated in Fig.14 (b). The specifications for the remote control [18] are listed in Table 11.

Fig.14. (a) FLYSKY FS-i6 (transmitter/receiver) (b) The control of a single channel

The remote control uses a Gaussian frequency shift keying modulation (GFSK) which is a form of frequency shift keying (FSK) as the digital data of form 0's ('logic low' or 'spaces') and 1's ('logic high' or 'marks') are encoded as continuous changes in carrier frequency. The data are fed to FSK modulator circuit, where the signal is modulated and then transmitted. However, in GFSK, the digital signal which is composed of -1 and 1 are fed into a Gaussian filter before they go into the FSK modulator. The Gaussian filter is used to reduce spectral width, by confining the emissions to a narrow spectral band. Moreover, this Gaussian filter helps to reduce the side bands power allowing smoother pulses which in turns reduces the possibility of interfering with neighboring channels.

DOI https://doi.org/2024-JICS-22432 | Generated on 2025-04-05 22:12:07

TABLE 11. FLYSKY-I6 REMOTE CONTROL SYSTEM SPECIFICATIONS

Transmitter parameters		**Receiver parameters**	
Manufacturer	FLYSKY	Number of channels	6
Model	FS-i6	Operating frequency	2.4GHz
Number of channels	6	Modulation type	FM – GFSK
Operating frequency/ Bandwidth	500KHz	Frequency range	2.405GHz-2.475GHz
Modulation type	FM – GFSK	RF receiver sensitivity	-105dBm
Radio frequency range	2.405Ghz-2.475GHz	Size	40.4 x 21.1 x 7.35 mm

As alluded earlier, the remote-control unit has 6 channels in which 4 channels will control the robot arm servos and 2 channels will control the main motors; i.e. : CH 1: Robot clockwise & C-clockwise move, CH 2: Robot forward and backward movement, CH 3: Arm joint 1 movement, CH 4: Gripper movement (open and close), CH 5: Arm base rotation (CW and CCW), and CH 6: Arm joint 2 movement. Although the entire pins of the receiver can be interfaced with the Arduino MCU to be programmed to control the servos, it is more efficient to connect the receiver pins directly to the servos when it is possible which offers better utilization and integration of the circuit. Also, the main motors must move backward and forward, it is not possible to maintain such a mechanism without the use of H-bridge motor control circuit. H-bridge circuit is used to control the rotation direction of DC motors (to be discussed further later). The signal will be received and sent to Arduino for processing. H-bridge circuit requires 4 control inputs which will be provided by Arduino to control the motors, the 6-channels 2.4GHz receiver configuration along with channels description is provided in Fig.15.

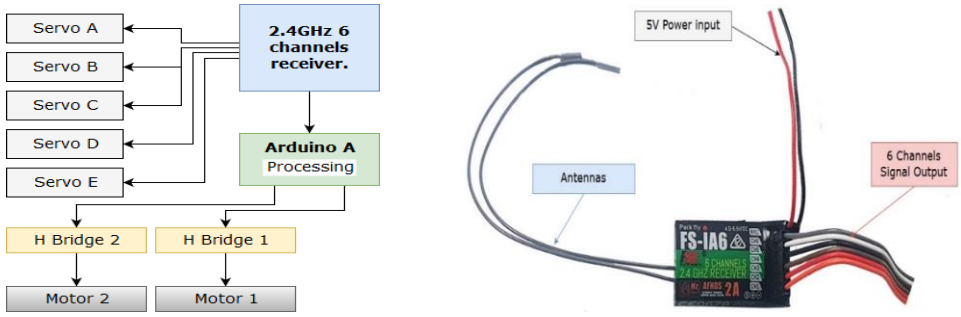

Fig.15. (a) Remote control circuit block diagram. (b) The 6-Channels, 2.4GHz receiver connections.

4.2. Wireless Communication Unit

A multi-channels radio frequency communication module has been implemented for the robot to obtain useful information from the sensory units. Thus, HC-12 SI4463 wireless transceiver module has been use in our design as it has different key features such as: it requires only +5VDC with maximum current 80µA - 16 mA to operate, its frequency band is 433.4 - 473.0 MHz with over 100 communication channels, it's a half-duplex serial wireless module with long wireless transmission distance of up to 1000 meters in open spaces, it transmits maximum power of 100 mW (20 dBm), and the receiver has a sensitivity of 2×10-15 W (-117 dBm) [18]. In addition, HC-12 SI4463 contains 9-pins and an external antenna that can be added to the module to enhance the communication range. Fig.16 demonstrates the HC-12 SI4463 chip along with major pins configuration.

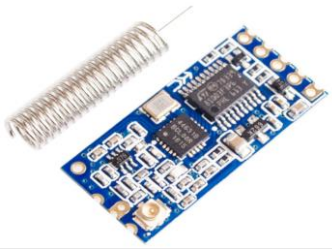

Pin Number	**Description**
1	VCC: Power supply input
2, 7 and 8	GND: Common ground
3	RXD: Input pin
4	TXD: Output pin
5	SET: Parameter setting control pin
6	ANT: 433 Hz antenna pin
9	No connection
ANT1-ANT2	External Antennas

Fig.16. HC-12 SI4463 wireless module and its pins configuration. [19]

This module was used for communication between two microcontrollers, one at the transmitting end and one at the receiving end. At the transmitting end, the module is connected to Arduino, which is connected to several sensors. The Arduino will receive, process, and transfer the sensors measurements to the wireless module, where it will be transmitted to the base. Fig.17 illustrates the connection channel between the wireless modules to MCUs.

Fig.17. Block diagram of the communication channel between the two Arduino Uno.

4.3. Camera Module

The use of camera in support of SRR will enable the system controller to monitor the field in a real-time system. Thus, we have decided to equip our SRR design with First Person View camera (FPV) [20]. FPV camera provides a real-time image that broadcasted through a video transmitter. It can also provide live videos and can record videos as files for later viewing. In addition, FPVs are small, lightweight and cheap which make them easy to integrate into various applications. Fig.19 illustrates the basic FPV setup.

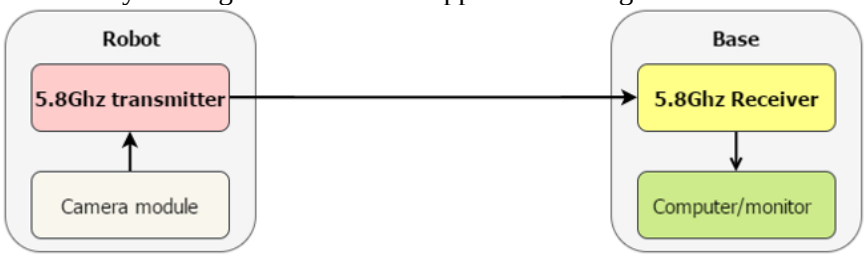

Fig.18. Block diagram if the communication system of the FPV camera module.

Selecting the appropriate FPV can be affected by several factors such as latency, resolution, and field of view. The latency of FPV camera is caused by the processing all the information from the image sensor where the faster processing the lower latency. Also, most of FPVs work on analog videos and their resolution are measured in TV lines (TVL) instead of measuring it in pixels which is common with digital video. Moreover, the field of view parameter measures the angel of view to locate objects. Finally, the dynamicity of FPV dictates how well the camera can record the details in very dark and very bright areas of an image. An IR cut filter block out any infrared light from reaching the camera sensor [24]. Thus, after researching various types of FVP modules, we selected 700TVL CMOS FPV camera, which comes with its own transmitter (transmitting frequency of 5.8 GHz). Table 12 represents the specifications of 700TVL COMS FPV camera along with video transmitter specifications [21].

TABLE 12. THE 700TVL COMS FPV CAMERA MODULE SPECIFICATIONS.

Specifications of 700TVl COMS FPV module		**Specifications of the transmitter.**	
Part name	700TVL CMOS FPV	Part name	TS5823 Wireless Aud/Vid Transmitter.
Lens	2.8mm Glass Lens	Working frequency	5645-5945Mhz
Voltage	12V DC+-5%	Power input	7-24V
Working current	70 mA	video formats	NTSC/PAL
Working temperature	-20C - 60C	Transmitting current	190mA 12V
Resolution	700TVL	Video band width/Audio coding	8M / 6.5M
Video output	1.0Vp-p/75ohm	Mass	7.3g (excluding antenna)
Mass	0.030 kg	Antenna connection	RP-SMA jack (TX module)

Finally, we have installed the camera on the robot's arm to give more freedom and better view and the transmitter was placed inside the robot for protection and to improve the general look of the robot. Fig.19 shows the camera/transmitter connections, camera placement, and transmitter connection respectively.

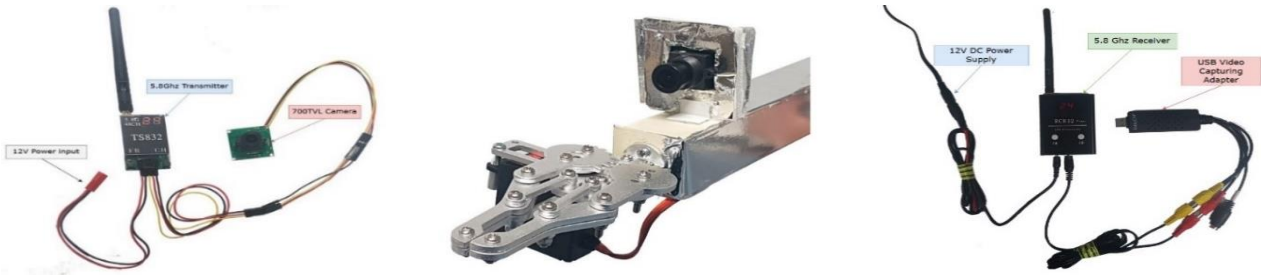

Fig.19. Camera & transmitter connection (b) Camera placement on the arm (c) Receiver components arrangement.

Note that the transmitter and receiver must have the same channel. In this design, channel 24 was set in both devices. The USB video adapter allows the user to view and record the video obtained from the camera directly to the base computer through a software provided by the manufacturer as shown in Fig.20 which shows a camera view for one of our labs.

Fig.20. The camera views

4.4. Gas Sensors

In current technology scenarios, monitoring of gases produced is very important. From home appliances, such as air conditioners to electric chimneys and safety systems at industries monitoring of gases is very crucial. Gas sensors are very important part of such systems. Gas sensors spontaneously react to the gas present, thus keeping the system updated about any alterations that occur in the concentration of molecules at gaseous state. Gas sensors are available in wide specifications depending on the sensitivity levels, type of gas to be sensed, physical dimensions and numerous other factors. Choosing the type of sensors to install is determined by where we want to send the robot. If the robot is intended to be sent to mines, then it must be able to detect gases that are most likely to be in mines, such as methane. Therefore, as SRR focuses on missions located in mines, factories, and buildings where fire is present [22], we will use a Gas Sensory Module to detect the most common gases as listed in table (17). Our gas sensory module consisted of four MQ-Series gas sensors.

TABLE 13. TARGETED GAS SENSORS MODULES AND SPECIFICATION.

Targeted gas	**Module Code**	**Gas presence**	**Normal value**
Carbon dioxide (CO_2)	MQ-2	During fires.	9
Liquid Petroleum Gas (LPG)	MQ-9	Homes, factories, industrial facilities.	24
Methane (CH4)	MQ-5	Mines, factories, industrial facilities.	10
Ammonia (NH3)	MQ-135	Factories, industrial facilities.	24

Each gas sensor has 4 pins: Vcc, ground, digital output, and analog output. In our case, the analog pin will be used, since it provides ability to obtain readings in terms of voltage levels as will be demonstrated later. Digital output only indicates the presence of the gas in terms of 0 or 1. In ordered to get accurate measurements, gas sensors must be ON for some time until the readings become stable. After running the gas sensors for some time, the readings were stable, in which the team has considered these values as reference values for normal conditions.

4.5. Ultrasonic Ranging Module

Since the robot tend to navigate around designated disaster and to measure distances within 2-3 meters at most, ultrasonic sensor module HY-SRF05 was used for ranging. HY-SRF05 operated by 5VDC (15mA) and provides distance measurement of a range of 2cm- 400cm (accuracy ±3 mm). Ultrasonic sensor waves are not affected by external factors, such as: sunlight, color of the obstacle, shape of the obstacle, therefore, it provides excellent measurements of distance. Fig.21 (a) shows the front view of HY-SRF05 module which contains all the necessary components needed for ultrasonic ranging function, such as transmitter, receiver, and control circuit.

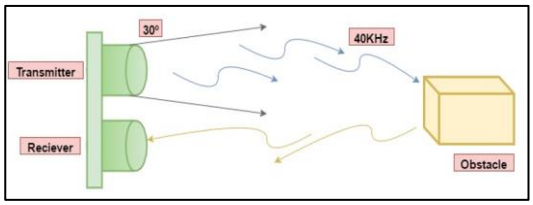


```
Distance: 32
Distance: 32
Distance: 31
Distance: 30
Distance: 33
Distance: 30
Distance: 32
Distance: 30
```

Fig.21. (a) Front view of HY-SRF05 (b) Demonstration of the ultrasonic module operation (c) sample readings

To start the measurement process, the module must receive a 'high' or '1' to its 'trig' pin for at least 10 µS. The transmitter end will emit eight cycles of ultrasonic pulses at 40 KHz which travels through the air, and if there was an object on its path, the signal will be reflected to the module. Note that the transmitter will transmit the ultrasonic signal at an angle of 30º, therefore, it can detect all the objects within 30º angle. If there was a reflected signal, the receiver end of the module will detect it and send a 'high' signal to the 'echo' pin. Once the 'trig' pin is set to 'high', a timer will calculate the time duration when the signal is sent, and when the signal is detected. This time duration is referred as travel time [23]. The graphical demonstration of the operation of ultrasonic module along with sample readings are illustrated in Fig.22(b/c). The distance between the sensor and the obstacle:

$$D = 1/2\ x\ Travel\ time\ x\ Speed\ of\ sound\ (340.29\ m/s).$$

Specification of the AM2320 sensor.	
Parameters	**Value**
Operation voltage	3.1V-5.5V
Current consumption	350 uA
Temperature scale	Centigrade
Temperature Accuracy	+-0.5C
Temperature range	--40 - 100 C
Humidity range	0% RH- 99.9%RH

```
Temperature: 21.10
Humidity: 35.40
Temperature: 21.10
Humidity: 35.60
Temperature: 21.20
Humidity: 35.50
Temperature: 21.20
Humidity: 35.50
```

Fig.22. Physical shape and specifications of A2320 sensor along with sample measurements.

4.6. Temperature and Humidity Sensor

Temperature and humidity sensors are important addition to SRR to provide additional measurements about the target area. AM2320 temperature and humidity combined sensor was integrated in the proposed SRR. It is capable of measuring temperatures from -40 C° up to 80 C°. In addition, it is easy to interface with the Arduino, since it requires no external circuitry and the output pin of the sensor is connected directly to the Arduino. Fig.22 demonstrates the physical shape and specifications of the sensor [24] along with sample simulation readings. Note that A2320 sensor contains four pin connections: P1 for Vcc, P3 for GND and P2/P4 for Signal.

4.7. Motor Driver Circuit

In this work, we have used a DC-Motor along with motor controller (i.e. H-bridge) to control speed, current and direction of motor. H-bridge is an electronic circuit that is used to apply voltage on a load such that the voltage's effect in terms of direction may be altered. Typical H-bridge unit is constructed by having four switching devices, mostly transistors and diodes, connected to a motor as illustrated in the Fig.23(a). as seen in the figure, the notations Q, D, M represents a transistor, diode, and the load M is a motor respectively. The top of the bridge is connected to a power supply and the bottom of is grounded. All switching transistors can be controlled to enable motion of the motor's shaft, and the direction of rotation may also be altered by the switching process as well. In Fig.23(b), the arrangement of turning on both Q1 and Q4 resulted in motion of the motor in a certain direction since the left side motor is at a higher voltage

than the other side. In contrast, in Fig.23(c), the voltage is applied in the reverse direction and the motor runs in the opposite direction now since Q3 and Q2 are turned on [25].

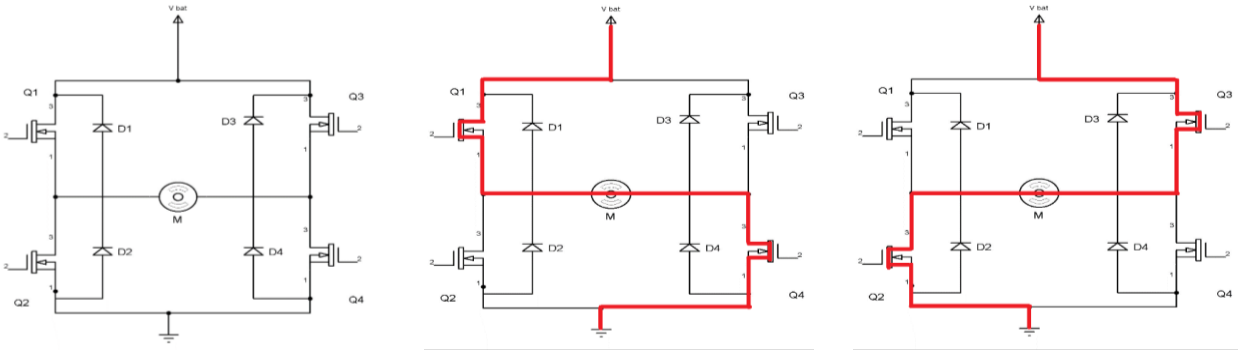

Fig.23. (a) An H-bridge constructed of transistors and diodes connected to a motor (b) H-bridge determining the direction of rotation for a motor (c) H-bridge operating the motor at an opposite direction of (b)

Practically, we have used L298N dual H-bridge module. Note that the L298N module need input voltage of DC 5-35V and supports 2 channels with maximum current per channel of 2 A, however, one channel was used only. This because the power consumed by the motor is around 25W, and the module can supply up to 25W. Thus, the team installed two modules, so each motor has dedicated h-bridge module. The H-bridge will be connected to Arduino A and to DC motor as demonstrated in Fig.24.

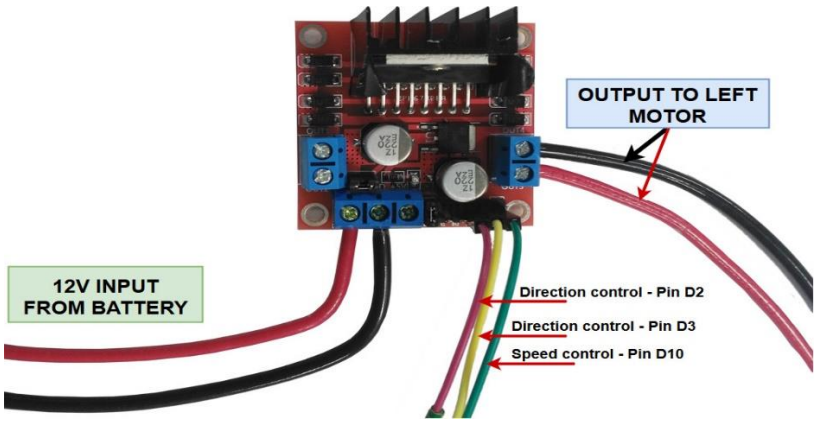

Fig.24. The actual implementation of the L298n H-bridge module.

The Arduino receives a signal from two channels connected to two digital input pins. It then processes the received signal and send low or high signals to the h-bridge pins. The H-bridge chip receives four inputs from Arduino to determine the rotation direction of the motors. Table 14 demonstrates the required signals states (1s and 0s) to move the robot to different directions. Although H-bridge module has four signal outputs, only two of them will be used (output 3 and 4).

TABLE 14: TRUTH TABLE FOR THE POSSIBLE MOVEMENT DIRECTIONS OF THE MOTORS.

Motor	H-bridge	H-Bridge Pins	Forward	Turn right	Turn left	Stop	Backward
Right	H-bridge 1	IN3	1	1	0	0	0
		IN4	0	0	1	0	1
Left	H-bridge 2	IN3	1	0	1	0	0
		IN4	0	1	0	0	1

4.8. Control Unit

The control unit is the brain of the system, in which it controls, regulate and link all the components of the system. The typical control unit can be built of using Arduino Microcontroller unit due to its attractive cost, features and ease-of-use. Arduino is an open source programmable MCU with free integration development environment (IDE) software that is used widely by amateurs and professionals to control small systems. Arduino boards can be easily interfaced with various components, such as, LEDs, servos, LDRs, sensors, DC motors. It can be easily connected to the computer via USB port to be programmed using C/C++ language and IDE software. Furthermore, Arduino boards are commonly available in three models: Uno, Nano, and Mega where each of which has its features and specifications. In

this work, we three Arduinos Uno to construct our control unit. Although a smaller and cheaper Arduino (such as Nano) could be used, Uno has better features & more pins, which allows for future development.

Arduino Uno is the most commonly used board as it equipped with Atmel ATmega328 microprocessor which is featured as high performance, low-power CMOS 8-Bit microcontroller along with 32Kb of flash RAM and 1KBytes EEPROM as well as 2KBytes Internal SRAM in addition to many other features [26]. As mentioned earlier, two Arduino Uno units (A & B) were installed on the robot while the third Arduino Uno is present and connected to a PC at the base station. These Arduino units were connected wirelessly through an RF transceiver chip to allow communication between the robot and the base in addition to transfer the sensory system information to the base. Arduino A (discussed earlier) is responsible of receiving signals from the remote-control receiver and controls the main motors accordingly. Arduino B is responsible of collecting the data from the sensors and transmit it to the base through the wireless module. Fig.25 demonstrates the circuit configuration for Arduino B along with the sensors. The component (U2) is the wireless module, which is connected to pin 7 of Arduino and the temperature sensor (U1) is connected to pin 6. Moreover, the four MQ series gas sensors are connected to analog pins A0 to A3, and the ultrasonic sensor is connected to digital pins D12 and D13. All the sensors operate on 5VDC; therefore, they are supplied from the DC-DC converter which has 5V output.

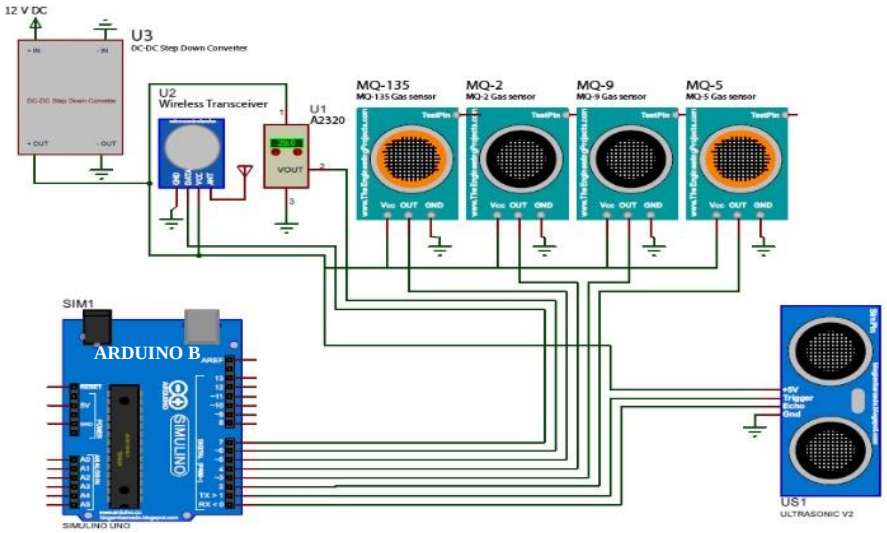

Fig.25. Arduino B circuit configuration.

4.9. Power Supply Unit

The robot contains of several electrical components, where some of them run on 5V and the others require 7.4V to operate. Since there is only one source of power: a 12V DC battery, voltage regulators were used to maintain the required voltages of the components. Instead of using conventional voltage regulators (as LM78055V) which have low efficiency and can withstand no more than 1 A, we have used a more powerful, reliable and effect adjustable voltage regulator.

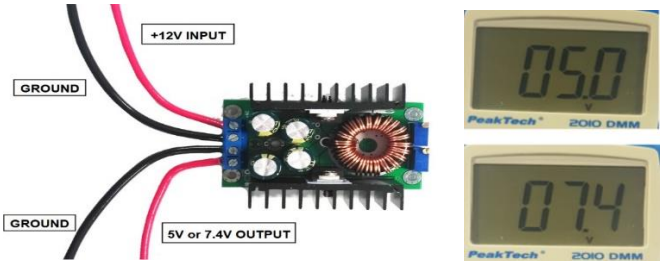

Fig.26. DC-DC Converter connections along with the measured outputs.

The DC-DC stepdown converter module can step down voltage from 5-40V to 1.2-35V and withstand up to 9A, 300W. It contains heat sink to dissipate heat from the chips. Thus, two DC-DC stepdown modules were used to supply 5V and 7.4V. These voltages satisfy the requirements of all the components of the robot. The connections of the voltage regulator are simple, since it has single high-voltage input, and low-

DOI https://doi.org/2024-JICS-22432 | Generated on 2025-04-05 22:12:07

voltage output as shown in Fig.26 along with the Multimeter measurement of both DC-DC stepdown converters' outputs.

4.10. Power Consumption

It is essential to calculate the power consumption ($P = IV$) of the robot in order to determine the battery capacity. Note that a 30% safety factor was assumed for the power consumption, due to various electrical losses. Due to the changes in some components of the robot, the actual power consumption has slightly changed from theoretical calculations. The actual power consumption readings are listed in Table 15.

TABLE 15. ACTUAL POWER CONSUMPTION OF THE ROBOT COMPONENTS.

Element	Voltage (V)	Current (A)	Power (W)	No.	Total Power (W)
Arduino Uno	9	0.050	0.45	2	0.9
Ultrasonic sensor	5	0.015	0.075	1	0.075
Gas Sensor	5	< 0.9	4.5	5	22.5
Temp sensor	5	0.025	0.125	1	0.125
15KG.CM Servos	7.4	1.5	11.1	3	33.3
20KG.CM servos	7.4	1.63	12.1	2	24.2
25 W dc motors	12	-	25	2	50
433MHz Wireless module	5	0.025	0.125	1	0.125
Camera Module	12	0.07	0.84	1	0.84
5.8 GHz Transmitter	12	0.19	2.28	1	2.28
Total Actual Power Consumption					**137.04**

From the table, it is observed that the theoretical calculations with a 30% safety factor predicted power consumption of 143.3 W, which was considered during the designing process. Due to the changes in servos types and DC motors, the actual power consumption has changed to 137.04 W. This value is within the design constrains of the project, which required a power consumption less than 200 W. Thus, the actual power consumption is 4.36% less than the theoretical calculations.

4.11. Battery

To estimate the required battery capacity, the run-time must be determined. Note that this robot is a prototype, and it will be used only for demonstration purposes. Therefore, it is assumed that this robot must run for a maximum of 40 minutes in the battery capacity. The battery capacity is measured in Ampere-Hour, or the power consumption in (watt-hours) divided by the system voltage. The equation of battery capacity is given by:

$$Battery\ Capacity\ (Ah) = \frac{Power\ consumption\ (w) * Time\ (h)}{System\ volatge\ (V)} = \frac{143.3\ * \left(\frac{40}{60}\right) h}{12} = \frac{143.3 * 0.67h}{12} = 8\ Ah$$

Thus, to achieve the robot run-time for 40 minutes, we need to employ a battery with approximately 8Ah. Also, the battery output current is an important concept for battery selection as it must be higher than the actual drawn currents to avoid damages in the system and the battery. By calculating the current drawn by each component, the total current drawn is approximately 12A. However, such values of capacity and output current is not available in markets, therefore, LONG 12V battery [27] with 8Ah battery was used. Now, as the available capacity of the battery is 18Ah, it can run the robot for longer period than the assumed. To estimate the operation time of the robot when it fully charged, we can use capacity formula as follows:

$$Battery\ capacity\ (Ah) = \frac{Power\ consumption\ (w) * Time(h)}{System\ volatge\ (V)} \rightarrow 18\ Ah = \frac{137.04W\ * T(h)}{12V} \rightarrow \boldsymbol{T(h) = 1.57\ hour}$$

Thus, the battery should be able to run the robot for 1.57 hour or 94 minutes. The battery can fit easily inside the robot container, and its mass is approximately 6.4 kg. The battery specifications are within the design constrains.

5. Design Construction

This section describes the hardware implementation phase where all the discussed components must be efficiently combined and connected in order to achieve the design objectives. For better readability, we will separate the discussion here into three major modules as discussed in the following subsections.

5.1. External Body Construction

The frame was constructed from aluminum as planned earlier. Six four-meter long aluminum straight angled plates were used. These plates were joined together using 8mm bolts to form two containers. Moreover, the same concept was adopted to build the entire robot. Joint corners formed very strong joints, which made the robot very rigid. The driving wheel teeth were slipping from the track. This problem was solved by changing the position of the driving wheel and the motor to the front. As a result, the driving wheel teeth could grip the track better. Fig.27 shows both the aluminum container and propulsion system respectively. It's clearly seen from the figure that the driving wheel now allows the track to make a 30-degrees angle with the ground. This allows the robot to drive and overcome small obstacles easily. In addition to fixing the position of the driving wheel, the arm was installed, and the servo motors have been placed as well as the method to rotate the arm base has been figured out properly. At this point, the robot frame was finished. In order to give it better look, the frame was covered with plastic lamination. Plastic lamination is a lightweight and strong material. Furthermore, it was then covered with shiny foil stickers to give it more industrial look.

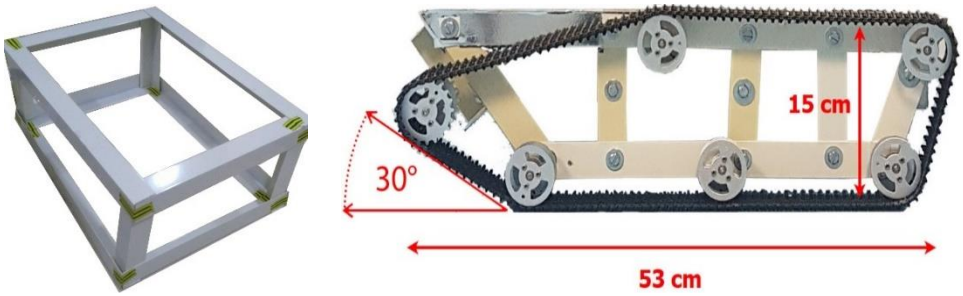

Fig.27. (a) Containers after joining the aluminum plates (b) Robot's propulsion system.

The final product of SRR is shown in Fig.28. The sensors were placed inside and in the front of the robot, to protect them from breaking or getting damaged. The battery is carefully placed in the center of storage area in order to have a proper center of gravity.

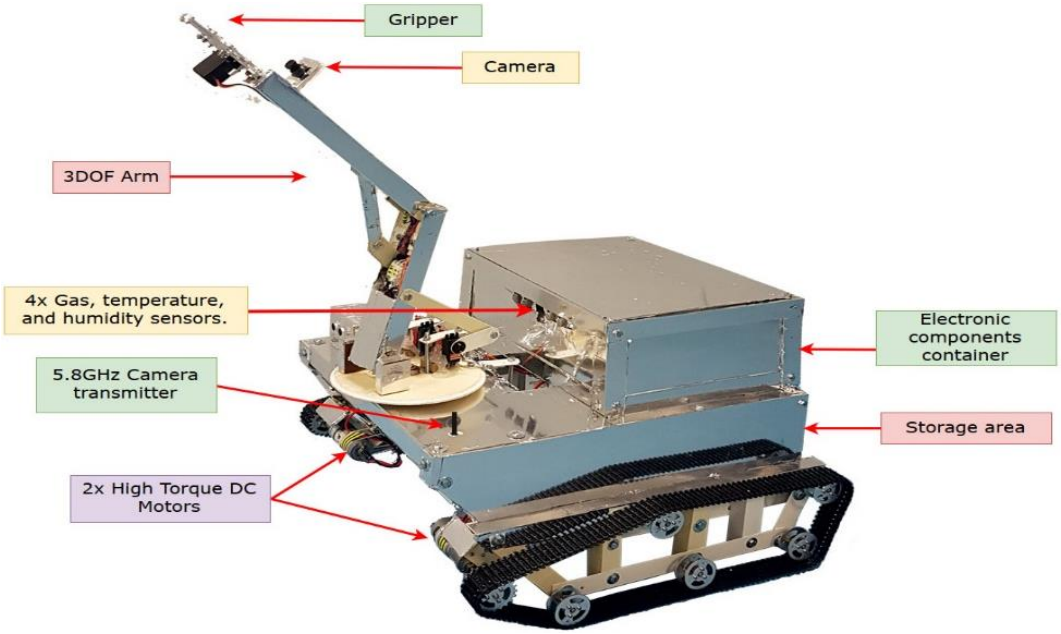

Fig.28. The Full Design of the Proposed Robot.

5.2. Arm Construction

The arm was implemented of 20 cm wooden disk base, which was held in place with two bearings and 8mm rod, to allow the base to rotate freely. The entire arm then was positioned on a rotating axel formed by joining two bearings and an 8mm rod as illustrated in Fig.29. This mechanism allows the arm to rest on the axel, and thus, the stress on servos was reduced.

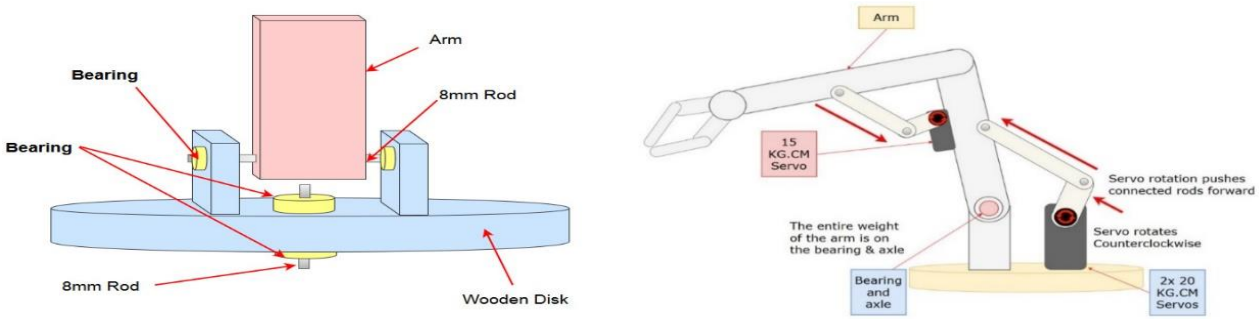

Fig.29. (a) Illustration of the arm concept (b) Arm movement mechanism

Implementing the arm to the servos directly resulted in too much stress on servos, which prevent them from lifting the arm. Note that the length of the arm was reduced slightly, since the length of the arm was more than needed. This improves the performance of the arm since it shorter arm require less torque to move it as seen in Fig.30.

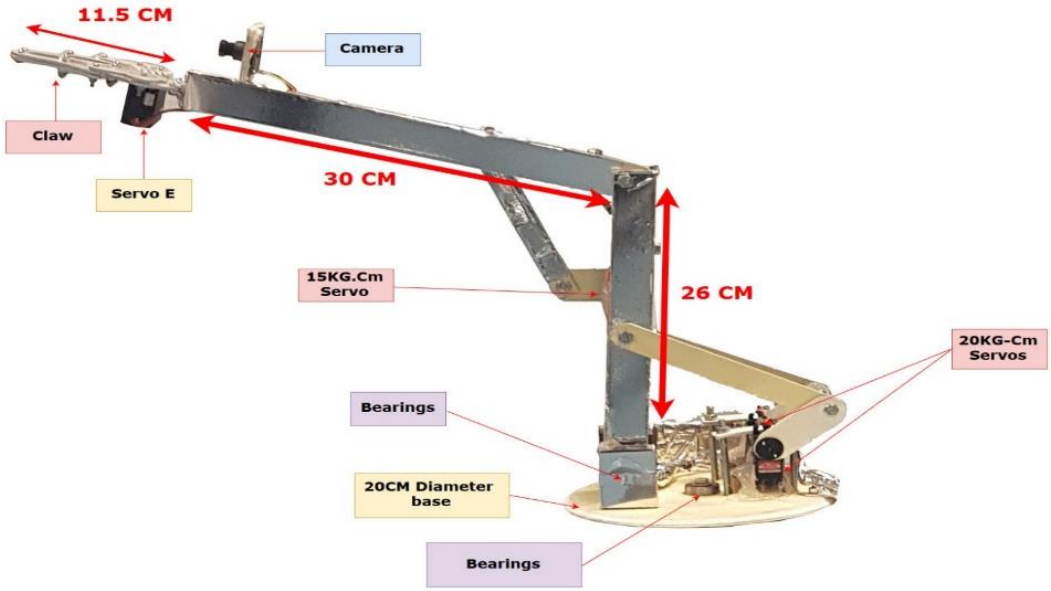

Fig.30. The components of the 3DOF arm.

5.3. Control Circuit Construction

The complete control circuit was accomplished by connecting all components, modules and wires. Due to the large size of the circuit, it was not possible to show all components in a single figure, instead, Fig.31 represents the actual circuit configuration while Fig.31 (b) shows the detailed circuit connection. Note that the camera module is not shown in the figure, since it only requires 12V supply, which can be obtained directly from the battery.

6. Design Coding and Configuration

The aforementioned hardware implementation to be efficiently utilized, it must be well coded and documented to operate as supposed. As mentioned previously, the robot's control units are composed of two Arduino Uno (A & B) which communicate to the base station through a user-friendly graphical interface. Therefore, the design coding phase can be divided into three major stages: The motion program (Arduino A), the sensor program (Arduino B) and the base station control interface program.

6.1. Arduino A - Motion Program

Arduino A receives the desired signal from the receiver and controls the motion of the robot and the arm accordingly. The readings are obtained from the 2.4 GHz receiver which is connected to Arduino A as demonstrated in Table 16. When the remote-control sticks are moved, the transmitter transmit certain value corresponding with the position of the sticks. By testing the remote control, we recorded out the

observations in Table 16 as reference values; therefore, threshold values were established to provide smooth motion. For example, if the stick of channel 2 moved upward until it sends value of 1700 up to 2000, the robot will move forward.

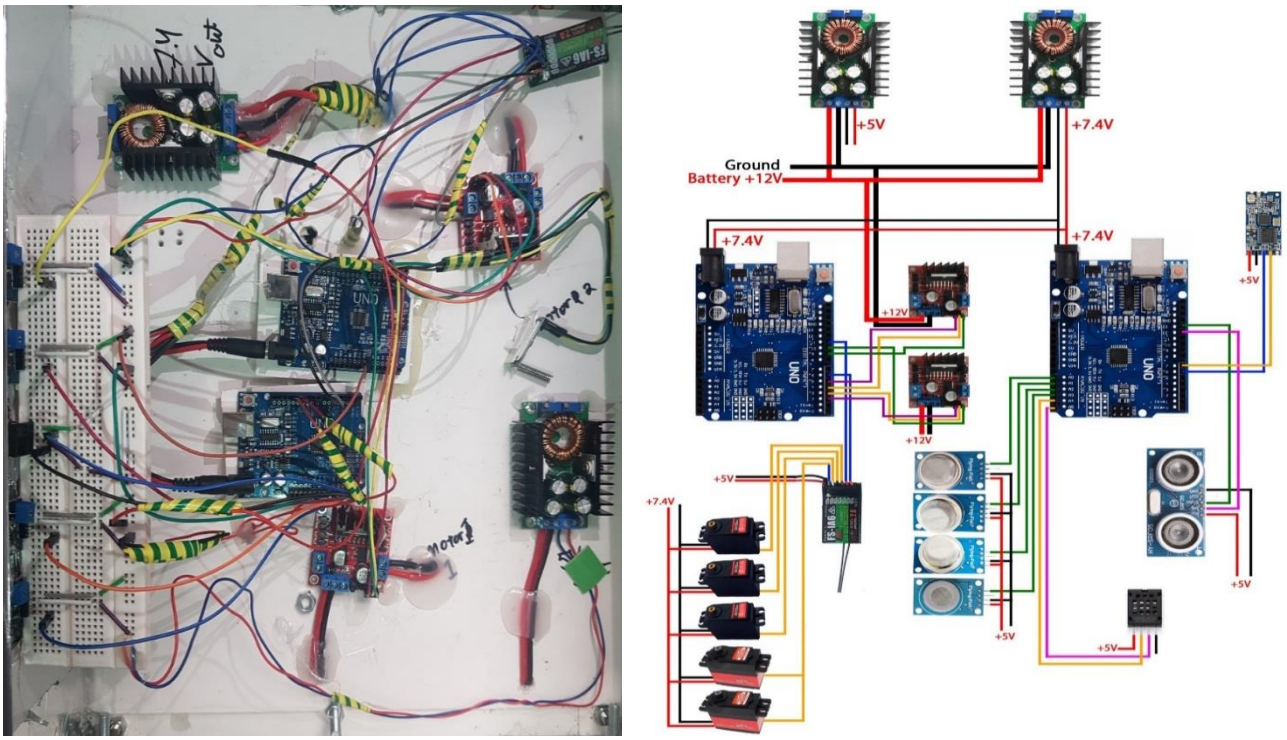

Fig.31. (a) Actual circuit inside the robot. (b) The final circuit diagram of the robot.

TABLE 16: THE MOTION OF THE TRANSMITTER STICKS AND THE CORRESPONDING SIGNALS.

Stick Placement	 Neutral	 maximum upward	 maximum downward	**The Required Motions With Its Corresponding Transmitter Values**		
				Motion	**Action**	**Transmitter values**
				STOP	Stick at Neutral	1201-1699
Arduino Readings	1580 1578 1580 1578 1579 1579 1580 1580 1580 1580	1971 1974 1974 1974 1977 1971 1974 1974 1971 1973	894 892 895 893 895 894 894 894 894 893	Move Forward	Upward	1700-2000
				Move Backward	Downward	900-1200

To develop the proper control program, the flowchart of the logic of motion was established for channel 2 which for the forward and backward motion and channel 1 for clockwise and counterclockwise rotations as in Fig.32.

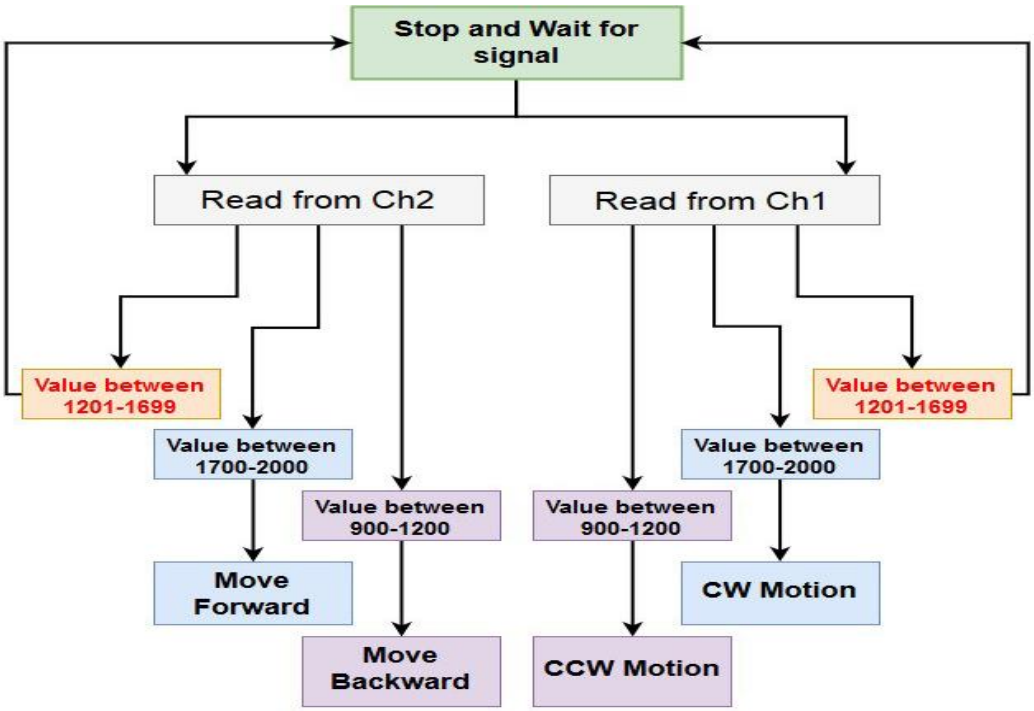

Fig.32. Flow chart of the code for Arduino A.

6.2. Arduino B - Sensors Program

Arduino B is concerned with reading the values of the connected sensors, processing the values, and finally transmit the readings to the base through the 433MHz transceiver chip. The flow diagrams of the gas sensors program and the ultrasonic sensor program are shown in Fig.33.

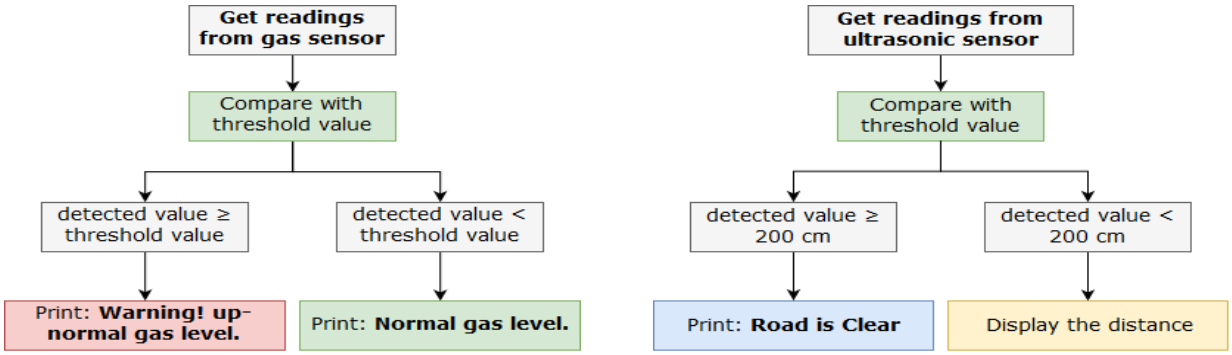

Fig.33. (a) Gas sensors program flow diagram (b) ultrasonic sensor program Flow diagram.

The sensor readings are dimensionless values, since they will be transmitted to the control station software such as the output results: 24, 40, 133, 32, 16, 104, 77). The base software will provide the necessary labeling and units. The results are arranged as follows: temperature, humidity, distance to nearest obstacle in cm, and four gas sensors readings. These values will be used in the next part to be displayed in more professional interface. The temperature and humidity are displayed directly. The gas readings are shown as numbers, which indicate the consternation of the gas in the air. But these numbers are pointless if they are not calibrated to real-life conditions. Therefore, a warning message will be displayed in case of high consternation of the gases instead of numbers. Also, the same principle was applied to ultrasonic sensor, where the program will display the distance to nearest object. However, of the distance is larger than 200 cm, the program will display “Road is clear” on the screen.

6.3. Control Station Software

Here, we have developed our user-friendly interface using MS-C#. Net programming language to read the measurements and display them in a more professional interface. The software reads the value from the serial communication port of the computer and display them in the GUI to a specific arrangement as shown in Fig.34.

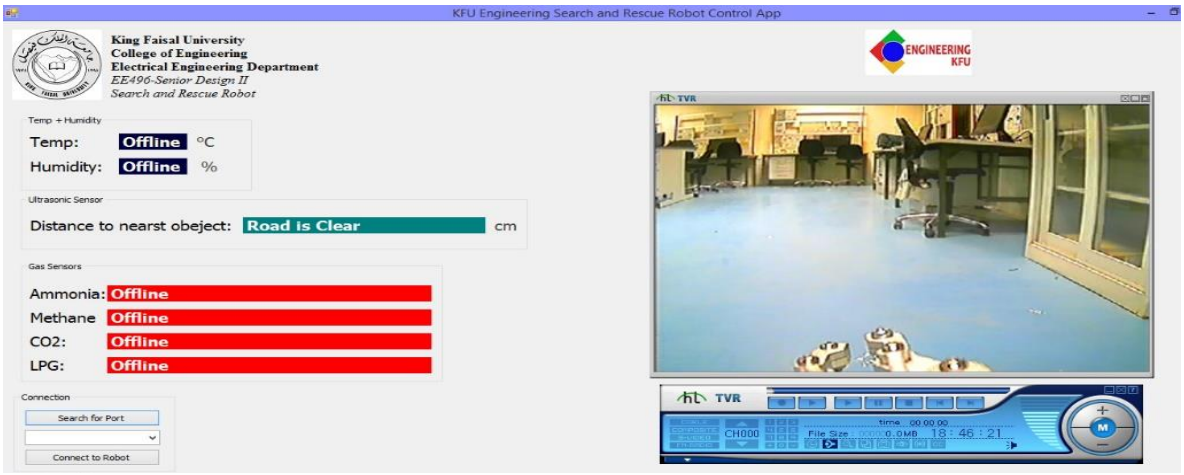

Fig.34. The graphical user-friendly interface of the base software

7. Design Testing and Evaluation

System evaluation phase is an essential phase of any system design life cycle in order to validate the system functionalities and provide a feedback report about every single component of the design. Therefore, we have established a set of parameters which are influenced by the functions presented in design constrains, such as: climbing small obstacles, detect humidity and temperature, conditions, gas detection, data transmission over distance, and power consumption. Note that all the sensors data and camera live feed were obtained wirelessly. As soon as you turn on the robot from the power switch, the robot will start the acquiring data from the sensors and transmit it to the base.

Climbing small obstacles: Since the robot is equipped with continuous track, it provides it with ability to climb various objects and obstacles. This function was validated by placing a 15-cm long piece of wood in front of the robot and observing its ability to climb it as shown in Fig.35.

Fig.35. Climbing small obstacles test.

Gas Detection: To test the gas detection functionality, gas sensors must be subjected to the target gases. Therefore, we have tested two gas sensors (LPG and CO2) since these gases were available in higher density. The test was done by using a lighter by leaking little amount of lighter's gas to check the detectability of sensors. This mechanism is illustrated in Fig.36. (a). Thus, the robot has detected the presence of LPG and sent the corresponding signal to the control station as seen in Fig.36 (b). Moreover, we have used the lighter again but in the firing state for a short period of time which supposed to cause the emission of CO2 gas. The results of this test are also given in Fig. 36 (c).

DOI https://doi.org/2024-JICS-22432 | Generated on 2025-04-05 22:12:07

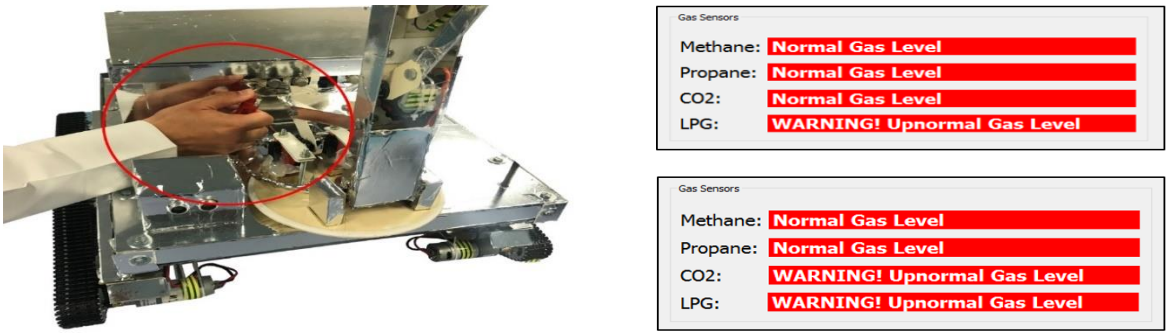

Fig.36. (a) LPG detection demonstration (b) Leaking Lighter's Gas Case (c) Firing Lighter's Gas Case

Distance Measuring: Distance measuring allows the person controlling the robot to know if there is enough space for the arm to be used, by indicating the distance to nearest obstacle. In the distance measuring test, a box was placed in front of the robot at 30-cm distance. This distance was measured carefully using a ruler. Also, we have measured the distance by the ultrasonic sensor via the base software and it shows the distance to be approximately 30-cm. Finally, when the obstacle is removed, the software will show that these is now obstacle by printing "Road is Clear" on the screen. The three scenarios (ruler distance, measured distance and empty road) are shown in Fig.37.

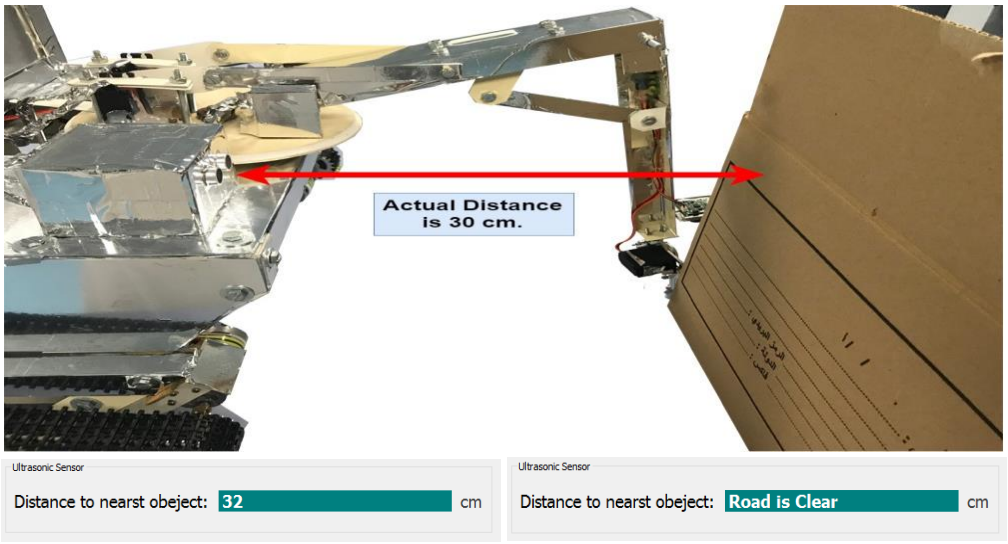

Fig.37. Actual distance, measured distance, Empty road of obstacle.

Detect Humidity and Temperature Conditions: This test was done by placing the robot in different conditions and observing the changes in temperature and humidity. Fig.37. demonstrates sample readings at the laboratory.

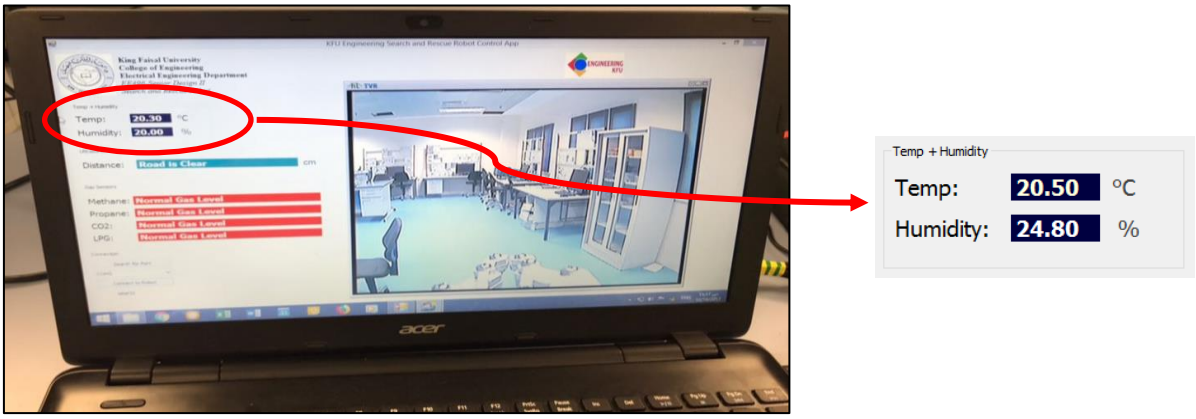

Fig.37. The control station during actual operation of the robot. Shows the temperature and humidity readings.

8. Conclusions and Remarks

Search & Rescue Robot (SRR) has been successfully designed, constructed and tested. It can enter dangerous zones and provide useful data for rescue team to help them understanding the condition of the zone without risking their lives. The proposed robot was extensively valuated in order to check its ability to perform the required tasks. It can ride on small obstacles and uneven surfaces and climb them successfully and carry weights up to 1 kg. The robot arm moves smoothly and steadily, and can carry weight up to 100 g. The arm design was changed several times and more powerful servos were implemented to it in order to improve its performance. Sensory system was tested too by subjecting gas sensors to the designated gases and observing the readings at control station computer. Temperature and humidity sensors were tested in various conditions to observe the reading changes. In addition, the proposed SRR robot has many interesting features that make it attractive and efficient such as:

- The robot size was engineered properly as it can enter tight areas and maintain stability when riding on uneven surfaces due to its low center of gravity.
- The robot frame was made of aluminum which provided it with strength and lightweights. The robot weighs 8.2 kg only without the battery which weighs 6.4 kg with storage capacity of 1 kg.
- It has two geared DC motors, each with a torque of 4.41 N.M (it requires only 2.53 N.M) and speed of 54 RPM. The increased torque improved the performance and provided ability for the robot to carry more weight. Every motor is connected to individual L298n H-bridge module to control the direction of motor rotation.
- The robot is powered by a 12V/18Ah battery which enable the robot to be operated for around 100 minutes. Also, the battery voltage is stepped-down to 5V and 7.4V to supply different electronic circuits.
- It contains two Arduino MCUs to control the robot motion and the sensory data processing and transmission. The motion of the arm and the entire robot is controlled by single remote-control through two 2.4 GHz R/C receiver channels that are processed by Arduino to move the robot in the desired direction and the other channels are connected directly to the arm servos. While, the sensory data are transmitted by 433 MHz module to another same module connected to Arduino at the control station computer.
- It has a camera mounted on the arm with wide angle, night vision, and wireless transmission capability. In addition to the user-friendly software application in the control station computer that can display all the data obtained from the sensors and the robot directly on the computer screen.

9. REFERENCES

[1]. IPB Inc. I. Saudi Arabia Mineral, Mining Sector Investment and Business. Washington DC: International business publications, 2015, pp. 116.

[2]. Council NR, Sciences DO, Board NS et al. Autonomous Vehicles in Support of Naval Operations. Washington DC: National Academies Press, 2005, pp. 49.

[3]. Murphy, R. Disaster robotics. Cambridge, Massachusetts: The MIT Press, 2014.

[4]. Bock, T. & Linner, T. Construction robots: "elementary technologies and single-task construction robots". New York, NY: Cambridge University Press, 2016.

[5]. Pohanish, R. Sittig's Handbook of Toxic and Hazardous Chemicals and Carcinogens. Burlington: Elsevier Science, 2011.

[6]. Kaufman, M. Mars landing 2012: inside the NASA Curiosity Mission. Washington, D.C: National Geographic Society, 2012.

[7]. Understanding the FCC Regulations for Low-Power, Non-Licensed Transmitters. Office of the Federal Register, 2010

[8]. Hatch, J. Aluminum: properties & physical metallurgy. Metals Park, Ohio: American Society for Metals, 1984, pp. 4-5.

[9]. Maitra, G. & Prasad, L. Handbook of mechanical design. New Delhi: Tata McGraw-Hill, 1995, pp. 3.16.

[10]. Avison, J. The World of physics. Cheltenham: Nelson, 1989, pp. 65.

[11]. Wong, J. Theory of ground vehicles. Hoboken, N.J: Wiley, 2008.

[12]. Pytka, J. Dynamics of wheel-soil systems: a soil stress and deformation-based approach. Boca Raton, FL: Taylor & Francis, 2013.

[13]. Sahin, F. & Kachroo, P. Practical and experimental robotics. Boca Raton: CRC Press, 2008, pp. 139-147.

[14]. Several servos from different online stores. Website. Available: www.aliexpress.com. Accessed: 1/5/2017

[15]. Kamm, L. Understanding electro-mechanical engineering: an introduction to mechatronics. New York: Institute of Electrical and Electronics Engineers, 1996.

[16]. Goodman, L. & Warner, W. Dynamics. Mineola, N.Y: Dover Publications, 2001.

[17]. High torque DC motor. Website. Available: www.aliexpress.com. Accessed: 1/5/2017.

[18]. FLYSKY FS-i6 User Manual. Website. Available: www.flysky-cn.com. Accessed: 3/5/2017.

[19]. HC-12 Wireless Serial Port Communication Module user manual, 2012. https://www.elecrow.com/download/HC-12.pdf.

[20]. Juniper, A. The complete guide to drones. New York: Wellfleet Press, 2016.

[21]. TS5823 5.8GHz wireless audio video transmitter and 700TVL COMS FPV Camera Product specifications. Website. Available: www.aliexpress.com.

[22]. Unal, A., Nayak, M., Mishra, D., Singh, D. & Joshi, A. Smart trends in information technology and computer communications: first International Conference. Jaipur, India, Singapore: Springer. 2016.

[23]. Lindgren, H., Santana, J., Novais, P., Caballero, A., Yoe, H., Ramirez, A. & Villarrubia,

[24]. G. Ambient intelligence: software and applications. Switzerland: Springer, 2016

[25]. Deshmukh, A. Microcontrollers: theory and applications. New Delhi: Tata McGraw-Hill, 2005.

[26]. ZHIPU high power dual H-bridge chip. Website. Available: www.aliexpress.com. Accessed: 5/5/2017

[27]. KEYKO KT-12180-HRT Cruzin Cooler Battery. Available via KEYKO. Website. Available: www.amazon.com.

DOI https://doi.org/2024-JICS-22432 | Generated on 2025-04-05 22:12:07